



Florian Beschliesser, BSc

FPGA-based verification of a narrowband receiver

MASTERARBEIT

zur Erlangung des akademischen Grades

Diplom-Ingenieur

Masterstudium Elektrotechnik-Wirtschaft

eingereicht an der

Technischen Universität Graz

Betreuer

Ao.Univ.-Prof. Dr. Erich Leitgeb

Institut für Hochfrequenztechnik

Mitbetreuer

Dr. Martin Gossar (NXP Semiconductors GmbH)

EIDESSTATTLICHE ERKLÄRUNG

AFFIDAVIT

Ich erkläre an Eides statt, dass ich die vorliegende Arbeit selbstständig verfasst, andere als die angegebenen Quellen/Hilfsmittel nicht benutzt, und die den benutzten Quellen wörtlich und inhaltlich entnommenen Stellen als solche kenntlich gemacht habe. Das in TUGRAZonline hochgeladene Textdokument ist mit der vorliegenden Masterarbeit identisch.

I declare that I have authored this thesis independently, that I have not used other than the declared sources/resources, and that I have explicitly indicated all material which has been quoted either literally or by content from the sources used. The text document uploaded to TUGRAZonline is identical to the present master's thesis.

Datum / Date

Unterschrift / Signature

Diplomarbeit

FPGA-based verification of a narrowband receiver

Florian Beschliesser

Institut für Hochfrequenztechnik

Technische Universität Graz

Leiter: Univ.-Prof. Dr. Wolfgang Bösch

In Kooperation mit

NXP Semiconductors GmbH



Betreuer: Ao.Univ.-Prof. Dr. Erich Leitgeb
Mitbetreuer: Dr. Martin Gossar (NXP)

Graz, im Mai 14

Abstract

This work was created in co-operation with the company NXP Austria GmbH and contains a FPGA based verification of a narrowband receiver using an analog frontend IC to gather the input ADC stream and a FPGA-evaluation board emulating the digital receive chain under test.

These verification setup should increase the test coverage of the prototypes before they are released for production. Furthermore the intense simulation time could be mitigated by using such a FPGA-based system.

Introductorily, the theoretical background of this thesis is discussed in detail. This chapter is split into two main parts: The analog frontend and the digital receive chain.

Afterwards the necessary hardware is introduced via block diagrams and detailed descriptions.

In addition the software environment and the TestStation project where this project should be integrated is introduced. In doing so, typical fields of application and potential users are discussed.

Finally the implementation is described in detail and the results are shown. Also a forecast of the portability of NXP products and applications in the future is given.

Kurzfassung

Diese Arbeit wurde in Kooperation mit der Firma NXP Austria GmbH erstellt und enthält eine FPGA-basierte Verifikation eines Schmalbandempfängers. Umgesetzt wurde das Projekt mit einem analogen Frontend-IC, um den ADC Strom zu erzeugen, und einer FPGA – Evaluierungsplatine welche die zu testende digitale Empfangskette emuliert.

Dieses Verifikationssetup soll die Testabdeckung der Prototypen erhöhen, bevor sie für die Produktion freigegeben werden. Weiters könnte die intensive Simulationszeit durch Verwendung eines solchen FPGA-basierten Systems gemildert werden.

Einleitend wird der theoretische Hintergrund dieser Arbeit ausführlich diskutiert. Dieses Kapitel ist in zwei Hauptteile aufgeteilt: Das analoge Frontend und die digitale Empfangskette.

Danach wird die notwendige Hardware anhand von Blockdiagrammen und detaillierten Beschreibungen vorgestellt.

Außerdem wird die Softwareumgebung und das TestStation Projekt vorgestellt, in jene das Projekt integriert werden soll. Dabei werden mögliche Einsatzbereiche und potentielle Anwender diskutiert.

Anschließend wird auf die Umsetzung genauer eingegangen, das Finale Ergebnis vorgestellt sowie ein Ausblick auf die Portierbarkeit auf neue Produkte und zukünftige Einsatzbereiche gegeben.

Table of Contents

1. Motivation and aim of the study	6
2. Technical background	9
2.1 Analog front end	9
2.1.1 Low noise amplifier (LNA)	10
2.1.2 Attenuators.....	11
2.1.3 Mixer	11
2.1.4 Baseband amplifier (TIA)	12
2.1.5 Automatic gain control (AGC)	13
2.1.6 Sigma delta ADC	13
2.2 Digital IF preprocessing.....	14
2.2.1 Decimation filter	15
2.2.2 DC notch filter	16
2.2.3 IQ mismatch compensation.....	17
2.3 Narrowband receive chain.....	17
2.3.1 Channel mixer.....	18
2.3.2 Channel filter.....	19
2.3.3 Demodulator	22
2.3.4 Clock data recovery	23
2.3.5 Data processing	26
2.4 Micro controller MRK3	28
2.4.1 Functional description	28
2.4.2 Monitor and download interface	29
3. Measurement procedures and standards.....	31
3.1 Receiver sensitivity.....	32
3.1.1 Method of measurement with continuous bit streams	32
3.1.2 Method of measurement with messages	33
3.2 Receiver jammer performance	35
3.2.1 Adjacent channel rejection.....	36

3.2.2	Co-channel rejection	37
3.2.3	Image rejection ratio	38
3.2.4	Image channel rejection	39
3.2.5	Blocking	39
3.2.5	Spurious response rejection.....	40
3.3	Modulation techniques.....	41
3.3.1	Frequency Shift Keying (FSK).....	41
3.3.2	Amplitude Shift Keying (ASK)	42
4.	Implementation	43
4.1	FPGA - Field Programmable Gate Array	43
4.1.1	Functional description	44
4.1.2	Hardware structure	44
4.1.3	Design and synthesis.....	45
4.1.4	Motivation for FPGA verification.....	46
4.1.5	Strengths.....	47
4.1.6	Weaknesses and limitations.....	48
4.1.7	Implementation effort	49
4.2	Hardware setup	52
4.2.1	Analog frontend.....	53
4.2.2	Level shifter board	54
4.2.3	FPGA evaluation board.....	55
4.2.4	Signal generator.....	56
4.2.5	Communication and modulation tool "TestStation"	58
4.3	Environmental software	60
4.3.1	TestStation firmware	61
4.3.2	Host software environment	62
4.3.3	Frontend IC firmware	63
4.3.4	Backend IC Firmware	64
4.4	Host software.....	64
4.4.1	Frame error rate measurement	65

4.4.2	Sensitivity measurement	66
4.4.3	Sensitivity test case	67
4.4.4	Enhanced sensitivity test case implementation	69
4.4.5	Signal to jammer ratio measurement	70
4.4.6	Interferer performance test case	70
5.	Results	73
5.1	Hardware setup	73
5.2	Configuration files	74
5.2.1	Sensitivity measurements	75
5.2.2	Jammer measurements	75
5.3	Result files	76
5.3.1	Sensitivity measurements	76
5.3.2	Jammer measurements	76
5.4	Result viewer	76
5.4.1	Sensitivity measurements	77
5.4.2	Enhanced sensitivity measurements	77
5.4.3	Jammer measurements	78
5.5	Excel export	79
5.5.1	Sensitivity measurements	79
5.5.2	Jammer measurements	80
6.	Conclusion and outlook	82
6.1	Comparison FPGA / IC	82
6.2	Capturing of ADC streams	83
6.3	Measurement time optimizations	83
6.4	Portability to future prototypes	84
	References	85
	List of Figures	87
	List of Tables	90
	Appendix A – RF frontend evaluation board	91
	Appendix B – FPGA evaluation board	92

1. Motivation and aim of the study

NXP Semiconductors Austria GmbH develops receiver systems since more than 10 years. Its main customers are placed in the automotive industry, such as Continental or Bosch. The main applications are car opening and immobilizing systems, where NXP provides several one-chip solutions for the key side, as well as for the car side. This means one single chip includes all the functionality for the application, no further microcontrollers or power amplifiers are needed.

The design of such receivers is split into two main parts: the analog front end and the digital back end. Both parts are essential for the performance of the final product and therefore big teams are working on each sub-block.

The analog design process is nearly the same since years. Taking the rough idea of a block as a starting point, first a schematic has to be developed. Afterwards an extensive and detailed simulation of all functions of the designed block has to be performed. Depending on the results, changes have to be done in the schematic and the simulation needs to be repeated again. Finally, if the results are looking fine, there are additional simulations over process and application corners performed, which should exclude the malfunction of this block under extreme conditions (e.g. extreme temperatures). Next to that, the analog layout of this block is drawn. The block design is finished, if the layout versus schematic simulation was pass. This simulation should detect possible function or parameter changes of the block caused by the layout. Like said before, this process is nearly unchanged since years. But this does not mean that the quality did not increase since years! The tools used for designing, simulating and layouting are improved periodically. The simulation results are more detailed, the simulation time gets less, displaying and reviewing the results is easier, etc. Therefore the design tools help the developers to work more efficient and produce high quality output.

Looking at the digital design process 10 years ago, more changes and innovations are visible nowadays. At least one thing did not change much: The Verilog or VHDL code is still typed into fancy editors most likely on an UNIX workstation. Maybe some intelligent code auto-completion system was introduced by some of the tools but in principal the way of working in the design phase is unchanged since years. Most of the innovations were happening in the digital design verification process. The main

verification solution is of course the digital simulation. Designing a test bench for a new digital block of the IC can require more working time than the design of the digital block itself. Nevertheless such a test bench is needed for every sub-block of the digital backend to prove its correct functionality. A digital block is called verified, if all possible input signal combinations were applied by the test bench. Each input signal combination should result in a certain output signal combination, the test bench should automatically compare the expected output with the simulated output and report possible errors. Exactly at this point one essential problem pops up: How does the verification look like, if the number of possible input signal combination is infinite, such as for the input of a receiver? How would you verify these blocks?

Looking at NXP Semiconductors, one possible answer to the question above is to introduce default use cases and a so called reference frame, which is an example of a modulated input signal fed into the digital receiver. All the simulations are done with this reference frame for all use cases. The use case defines the modulation technique, the modulation index and the chip rate of the input signal. The reference frame defines the encoding and the amount of the sent data. As you can imagine, the simulation coverage is quite low if you are just using one input frame and some chip rate / modulation index combinations. Unfortunately the simulation time is very high for such test benches, therefore the simulation coverage can't be increased easily. This limitation is also limiting the quality of the design itself, because a solid verification is the key to success in such design projects.

Considering the limitations of the simulation process above, there was a request for a faster, more effective way of verifying the digital sub-blocks of the receiver. A new idea, and also the topic of this study was born: **FPGA Verification**.

Aim of this study is to implement an automated test bench using an UHF transmitter, an analog front end and a field programmable gate array (FPGA) which is an integrated circuit that can be configured after manufacturing by the end customer. It contains the digital blocks of the receiver to increase the test coverage of the digital design. Not only one, but dozens of different input frames, using several use cases and modulation techniques should be tested. Additionally the test bench should provide functionality to simulate a second present transmitter in the working area of the receiver, meaning the interferer performance of the design. Very important is, that

the test bench is easily configurable, portable to any version of the digital receiver and able to produce well-structured result tables and plots.

2. Technical background

In this chapter the receiver to be verified is further explained. The functional blocks are split into two main parts: the analog and the digital part of the receiver. Following the signal path, the chapter will handle first the analog front end, afterwards the digital front end and finally the digital baseband processing which is the part that should be verified in detail. The complete system is shown in the diagram below.

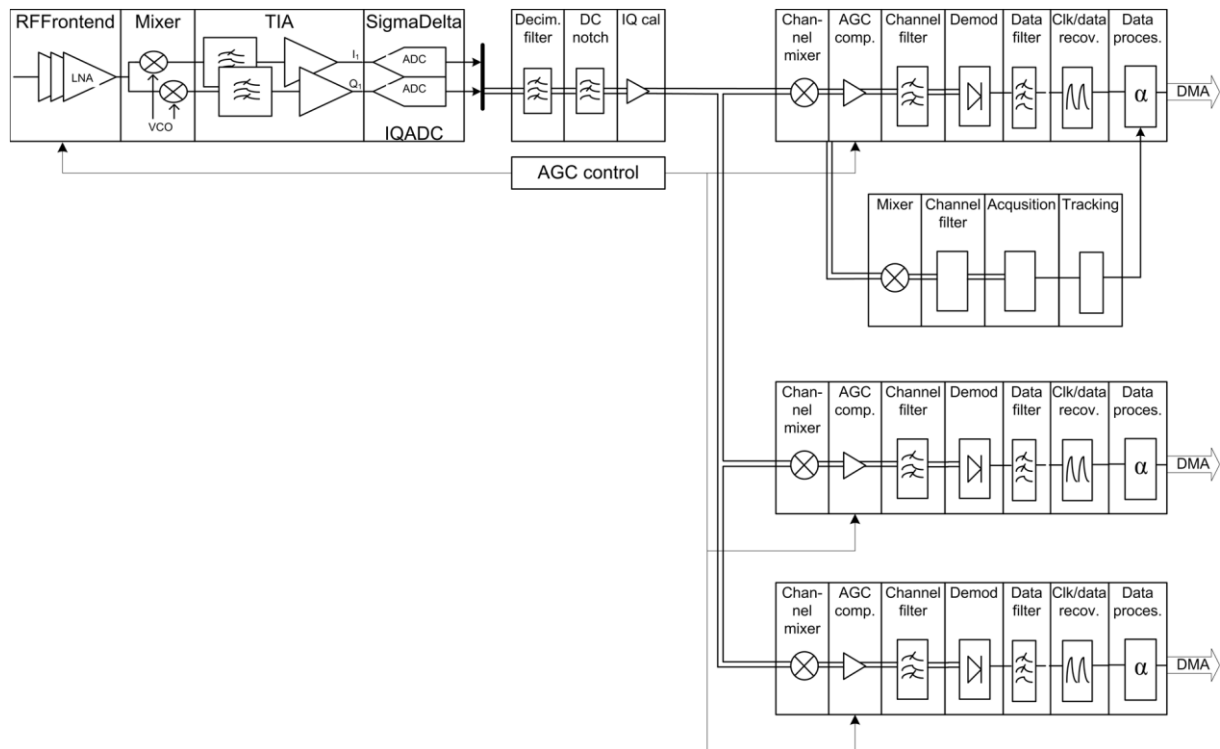


Figure 1: Full receive chain [1]

2.1 Analog front end

The UHF receiver is implemented as a low IF RF down conversion system. To provide the necessary dynamic range, low gain in the RF and a high resolution ADC in the baseband is used. The system includes a high linearity LNA stage, supported by passive attenuator blocks controlled by an AGC loop. Down conversion and high gain baseband amplifiers ensure that the dynamic range of the ADC is exploited fully. The digital receiver frontend is common to all receive channels and includes the preprocessing and I/Q compensation. The parallel digital receive chains perform the channel selection, demodulation and framing. The analog front end is shown in the next figure.

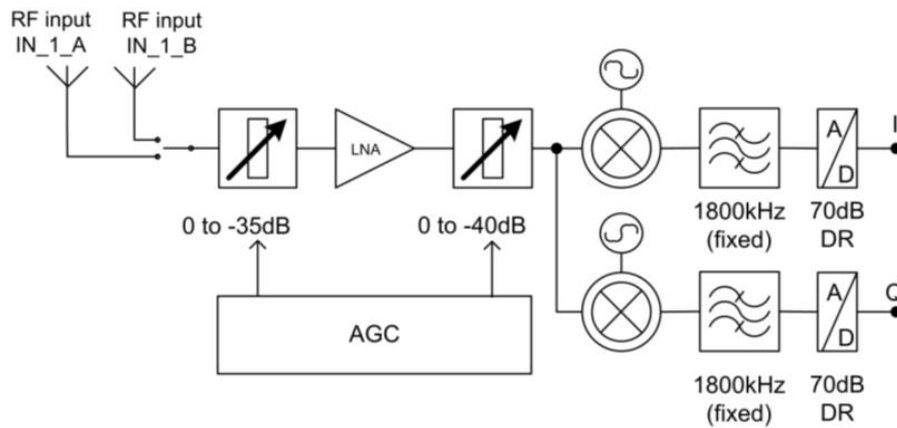


Figure 2: Analog Frontend [1]

The following chapters will explain the sub-blocks of the analog front end in detail.

2.1.1 Low noise amplifier (LNA)

A LNA is an electronic amplifier designed to amplify very weak signals such as from antennas. They are usually placed very close to the antenna output to avoid signal losses due to cables etc. The LNA is a key component in a receiver system, as per Friis' formula the overall noise figure of an analog front end is dominated by the first few stages [2].

By implementing a LNA, the amount of noise processed to subsequent stages of the receive chain is reduced by the gain of the LNA, while the noise of the LNA itself gets directly injected into the signal path. Thus, it is essential for a LNA to amplify the desired signal power while adding as less noise as possible, so that the signal to noise ratio of this signal is maximized in the later stages in the system.

When evaluating LNAs, there are three main parameters to look at: the noise figure, the gain, and the linearity. The noise figure expresses the difference in decibels between the output noise of the receiver to the output noise of an ideal receiver with the same overall gain and bandwidth. Both are theoretically connected to matched sources at the standard noise temperature (290K). Easily expressed, the noise figure is a value that defines the amount of noise that a device adds to a signal that passes through it. Therefore the noise figure is an often used figure of merit to compare different receiver performances [3].

The implemented LNA is a wideband inductor-free, highly-linear, low-power and low-noise amplifier. It uses internal feedback for obtaining its high linearity and a well-defined gain as well as good input matching over temperature and voltage. The LNA has a single-ended input with a wide-band input matching optimized for 200 Ohms.

2.1.2 Attenuators

Passive 2 dB step attenuators are positioned in front of the LNA and in front of the mixer in order to control the gain of the receiver. The input selection between the two antenna inputs is realized by the first attenuator. The radio frequency (RF) inputs have integrated electrostatic discharge (ESD) protection and integrated alternating current (AC) coupling for easy application. A matching network can be applied off-chip for best performance and adaptation to different source impedances.

2.1.3 Mixer

The implemented mixer is an IQ mixer. It addresses the problem of maximum information density in a limited bandwidth by allowing the user to modulate both the in-phase and quadrature components of a carrier simultaneously. The basic building blocks of IQ mixer are shown in the figure below.

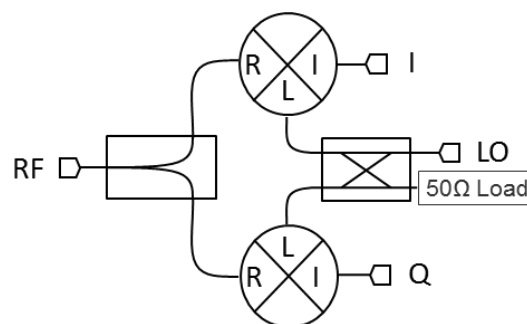


Figure 3: IQ Mixer [4]

An IQ mixer consists of two mixers with a local oscillator (LO) that is shifted by 90° to each other. During a normal down conversion the phase of the LO is irrelevant because the data will be single sided. The IQ mixer requires transmission of both sidebands for accurate reconstruction of the original signal.

The IQ mixer uses the basis of quadrature modulation, meaning it can be used to cancel out one of the two side bands, the image channel. By adding an extra 90° phase shift to the Q channel after mixing, a complete 180° phase shift will be created, leading to the inversion of one of the original signal components. Adding the two mixer output channel would now result in a cancellation of one component of the signal, while the other component is reinforced. This is called image rejection [4].

When an IQ mixer is used as a down-converter it allows both of the original data signals to be retrieved with an appropriately phased LO signal. The image channel is finally removed in the digital channel filter. A special algorithm is used to remove the impact of analog mismatch in the I and Q mixer on the image rejection, what normally would cause the intrusion of the image channel into the wanted channel.

2.1.4 Baseband amplifier (TIA)

The baseband amplifier stage amplifies the balanced quadrature (I and Q) mixer output signals to the optimal level for the analog to digital converter (ADC) and performs the anti-aliasing filtering in front of the sigma-delta ADC. Internal DC offset correction loops guarantees maximum image suppression and high linearity / dynamic range.

As the mixer output is a current, a transimpedance amplifier is used to amplify the signal and to convert the current into a voltage. The basic block diagram is shown in the figure below.

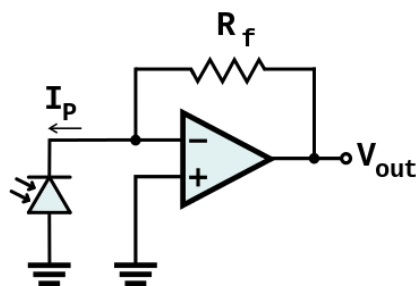


Figure 4: Transimpedance amplifier [5]

The TIA differs from the conventional operational amplifiers mainly by its low ohmic input. This means it is current controlled. In its simplest form a transimpedance amplifier has just a large valued feedback resistor, R_f . This resistor defines the gain

of the amplifier and because the amplifier is in an inverting configuration, the gain has a value of $-R_f$ Ohms.

Due to their characteristics TIAs are mostly used for amplifiers with high bandwidths (e.g. video amplifiers). Both, inverting or non-inverting feedback is possible [5].

2.1.5 Automatic gain control (AGC)

The automatic gain control (AGC) ensures that the analog frontend is protected from high power signals and therefore ensures high linearity figures throughout the whole dynamic range of the receiver.

The AGC measures signal strength, makes a decision to get the best performance and drives the gain of the analogue front-end. For measuring signal strength overload detectors are present at the LNA and at the TIA, and in addition the 1-bit ADC bit stream is monitored by a run-length detector. The overload detectors are fast response voltage comparators with reset control. The run length detectors, in the digital part of the AGC, allow the maximum ones or zeroes sequences to be used as a measure of the saturation of the ADC.

The AGC control strategy has been optimized for providing the best noise figure and maintaining all linearity requirements. Therefore the first steps of the attenuation are always done with the baseband (TIA) attenuator. The next steps are done with the frontend (LNA) attenuator until it has reached its maximum attenuation. The remaining attenuation steps are done with the baseband (TIA) attenuator again.

2.1.6 Sigma delta ADC

A modern Sigma Delta ADC works with an at least 64-times oversampling rate and with a resolution of 1Bit. The ADC consist out of two blocks: an analog modulator and a digital filter. The modulator is in principle just a comparator (delta) with a low pass as integrator (sigma) in front. At the same time, the back-converted output signal is subtracted from the input signal using a 1-Bit DA converter and a differential amplifier. This ensures, that the comparator is resetted after each bit. This is how a 1bit data stream is generated. If the amplitude of the input signal is rising, the output of the comparator is mainly "1", if it is decreasing, the output is mainly "0". By

integrating this bit stream (low pass), the analog signal could be regained immediately [6]. Following figure shows the block diagram of such a sigma delta ADC.

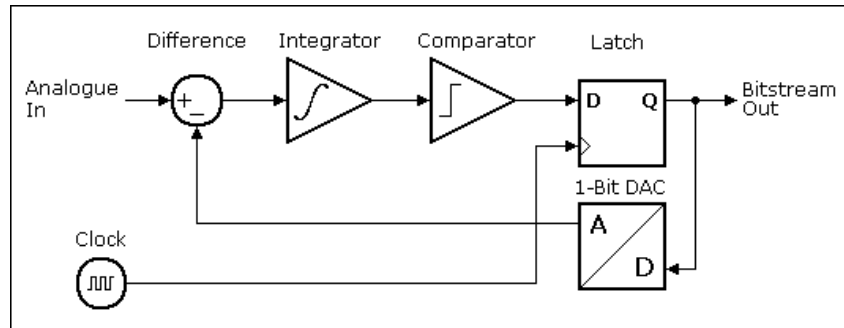


Figure 5: Block diagram of a first order SD ADC [1]

The implemented ADC is a 1-bit higher order oversampled SD-ADC. The output is a single bit data-stream which is further processed by the digital baseband.

2.2 Digital IF preprocessing

The IF pre-filter blocks performs sampling rate reduction from the high oversampled one bit sigma delta bit stream into a Nyquist sampling multi bit signal. Furthermore the decimated signal is high pass filtered to remove unwanted DC components which could disturb further processing in the IQ compensation unit. The IQ compensation unit removes the unwanted image frequency components from the complex low IF signal.

Following block diagram provides an overview of the contents of the digital IF preprocessing.

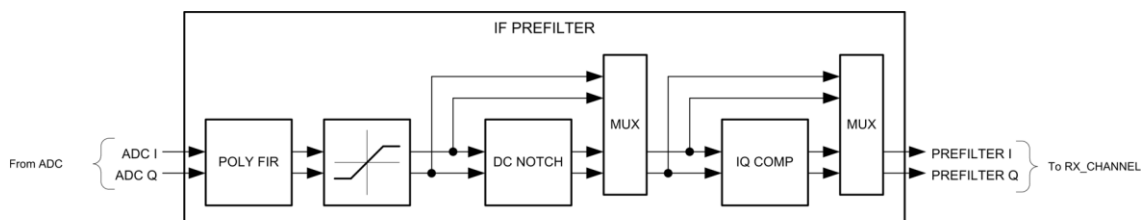


Figure 6: Block diagram of the IF preprocessing [1]

2.2.1 Decimation filter

The decimation filter restores the IF signal from the highly oversampled 1 bit data stream of the sigma delta ADC at a sample rate of 3.6 MS/s. The decimation filter has a fixed cut-off frequency of ~1 MHz with an almost flat pass band over the supported intermediate frequency range from -900 kHz to 900 kHz.

By feeding the output of the sigma delta ADC into the decimation filter, it has to fulfill three tasks: It has to filter out-of-band quantization noise, out-of-band signals present in the modulator's analog input and it has to lower the sampling frequency to a value closer to two times the highest frequency of interest.

The filter is realized by low pass filter followed by a down sampling unit like shown in the figure below. ωT_1 and ωT_2 indicate the different sample rates at the input and output, where $T_2 = T_1/M$. The downsampling rate in this formula is defined by the parameter M [7].

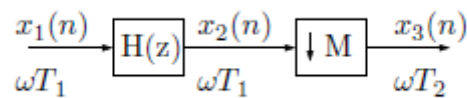


Figure 7: Decimation filter with lowpass filter followed by down sampling [7]

The lowpass filter is needed to limit the band to π/M , otherwise aliasing would occur. The filter will attenuate all frequency components from π/M to π . Following figure shows an ideal low pass filter with a cut off frequency at π/M [7].

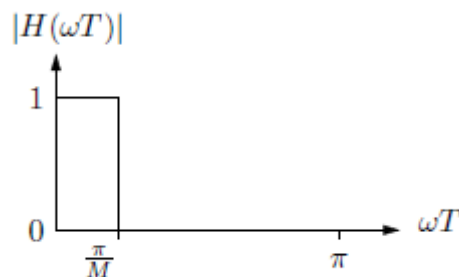


Figure 8: Lowpass filter with a cut off frequency of π/M [7]

The last step of the decimation is the downsampling by a factor M. This means that a new signal is created by selecting every M'th sample in the input of the

downsampling unit. All other samples are neglected. Following figure shows an example of a decimated signal [7].

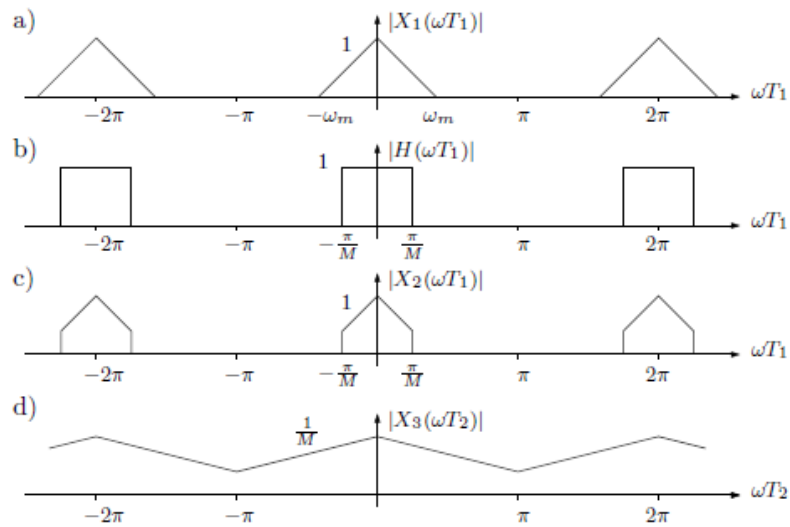


Figure 9: Example of a decimated signal [7]

The line a) in the figure above shows the magnitude response for the signal $X_1(\omega T_1)$ with the bandwidth ω_m . The Ideal lowpass filter with cut off frequency π/M is plotted on line b), while line c) shows the magnitude response for $X_2(\omega T_1) = X_1(\omega T_1) * H(\omega T_1)$ which is the filtered version of $X_1(\omega T_1)$. The last line shows the downsampled version of $X_2(\omega T_1)$. $T_2 = T_1/M$.

2.2.2 DC notch filter

The DC notch filter removes the DC gain introduced by the analog frontend. The use of the DC notch filter is optional in normal receive operation and can be bypassed. The DC notch filter is a second order filter with a stop band width of ~ 25 kHz (i.e. cut-off frequencies at -12.5 kHz and 12.5 kHz).

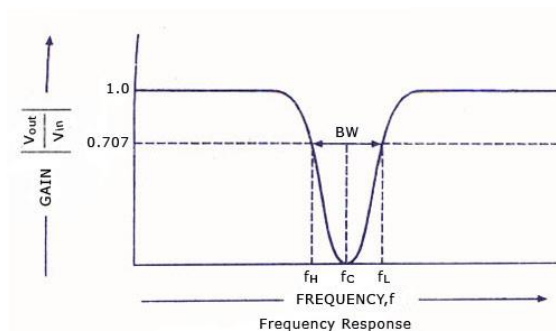


Figure 10: DC notch filter response [8]

2.2.3 IQ mismatch compensation

The analog tuner circuit has an in-phase and a quadrature (I/Q) path after the mixer. The imbalance of the mixers as well as the baseband performance of the I and Q channels lead to a variation of phase and amplitude of these signals. This causes insufficient suppression of the image frequencies. The contributions of the mismatch arise in the phase mismatch of the signals used for mixing, in the imbalances of the mixer itself, in the phase delays of the baseband path, in the gain errors of the mixers and in the gain errors of the baseband amplifiers as well as in the ADC input stage.

In order to have sufficient image suppression it is necessary to calibrate the digital baseband signals to compensate the errors of the analog paths. The phase and the amplitude errors are corrected in the baseband signal, processing centrally for all channels.

For fast calibration a test tone supplied either from external or internally generated is required for calibration. The purity of the calibration tone improves the accuracy and settling time of the calibration algorithm.

2.3 Narrowband receive chain

The narrowband receive chain gets its data from the intermediate frequency (IF) preprocessing and performs all remaining steps to demodulate the received data. First, the IF signal is mixed down to zero IF, afterwards the attenuator steps of the AGC are compensated. Afterwards the signal passes a configurable channel filter with a finite duration impulse response and finally it gets demodulated by a number of coordinate transformations in the demodulator. The gained demodulated signal is fed into the digital data processing for further handling of the input data. (e.g. direct memory access (DMA))

Following block diagram provides an overview of the contents of the narrowband receive chain.

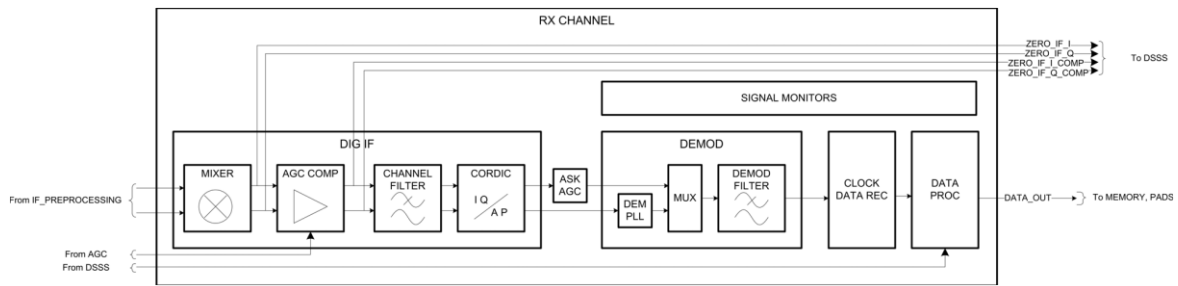


Figure 11: Block diagram of the narrowband receive chain [1]

2.3.1 Channel mixer

The channel mixer performs the remaining down conversion of the low IF signal to zero IF. It is used to select a band of interest in the received wideband IF signal. The successive receiver topology expects zero IF signals, hence the mixer must be configured correctly to allow the remaining signal processing chain to operate properly.

The mixer uses a CORDIC in rotation mode. The CORDIC algorithm was developed 1959 by J.E. Volder and 1971 extended to the actual used version by J.S. Walther. The abbreviation CORDIC stands for Coordinate Rotation Digital Computer [8]. This algorithm provides elementary trigonometric and hyperbolic functions using just fast operations like additions or shifts. This makes it possible to use sine and cosine functions in a digital environment for computing complex signals.

Following figure illustrates the CORDIC algorithm in progress. The starting vector v_0 is always $[1, 0]$. In the first iteration this vector is rotated by 45° counterclockwise to get the vector v_1 . Successive iterations are rotating the vector in positive or negative direction with size-decreasing steps, until the wanted angle has been reached. The step size is $\arctan(1/(2^i-1))$ for $i = 1, 2, 3, \dots$

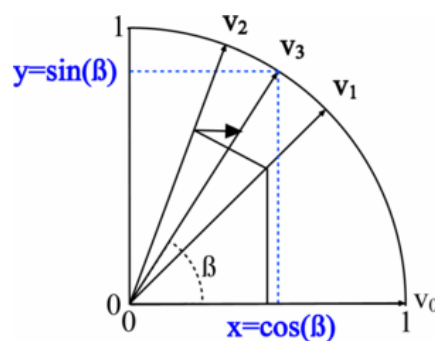


Figure 12: CORDIC algorithm process [8]

Due to the CORDIC principle the IF signal is shifted by a phase increment to the desired target frequency. Unlike other mixing principles this procedure does not introduce any unwanted mixing products.

The programmable mixing frequency of the receiver ranges over the entire IF bandwidth from -900 kHz to +900 kHz with a resolution of 100 Hz.

2.3.2 Channel filter

The channel filter allows the selection of a desired band of interest out of the wideband IF signal. The filter cut-off frequency is selected by a configurable sample rate conversion stage. For correct baseband operation, the maximum chip rate of the wanted signal must not exceed a certain value.

The channel filter is realized with an FIR filter using a windowing function [9]. The design of FIR filters using windowing is a simple and quick technique. The frequency response of an ideal low pass filter is shown in the figure below. The x axis is normalized to the sampling frequency. The transition frequency is always between 0 and 0.5, as 0.5 represents the Nyquist frequency. As expected from a low pass filter, all frequencies below the cut off frequency are passed, where-as all frequencies above are rejected.

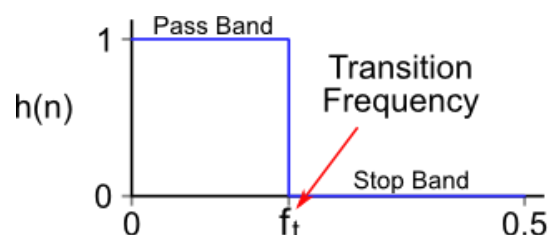


Figure 13: Ideal low pass filter [9]

The sinc function shown below is the impulse response of this ideal low pass filter. If it would be possible to create filters with this impulse response, one could build a filter with a frequency response like shown above [9].

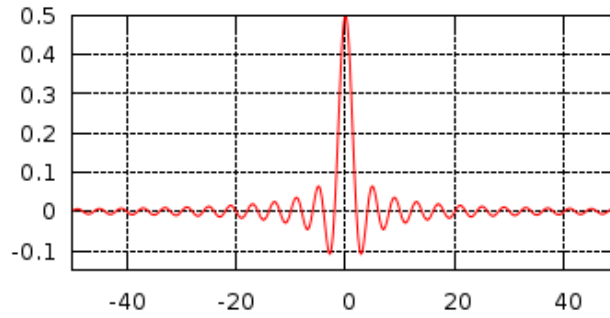


Figure 14: Impulse response of ideal LPF [9]

Unfortunately it is not as easy as that. In fact, there are two problems with creating this ideal impulse response.

First, the sinc function is infinite in the x direction, the ideal filter would require an infinite number of taps. However, the finite impulse response (FIR) filter only allows us to create finite impulse responses, the number of filter taps must be finite. Second, the impulse response is non-causal, which means that an implementation would require samples from the future.

Luckily, there are solutions for both issues available. First, a window is applied to the sinc function such that only a part of the impulse response is used. Furthermore, the impulse response is shifted in a way that the filter only operates on available samples. Following figure shows how only a part of the sinc function is used for the filter design. The filter length of following example is 21 weights, which results in a filter order (M) of 20. The cut off frequency of this example is 560 Hz, the sample frequency is 2000 Hz.

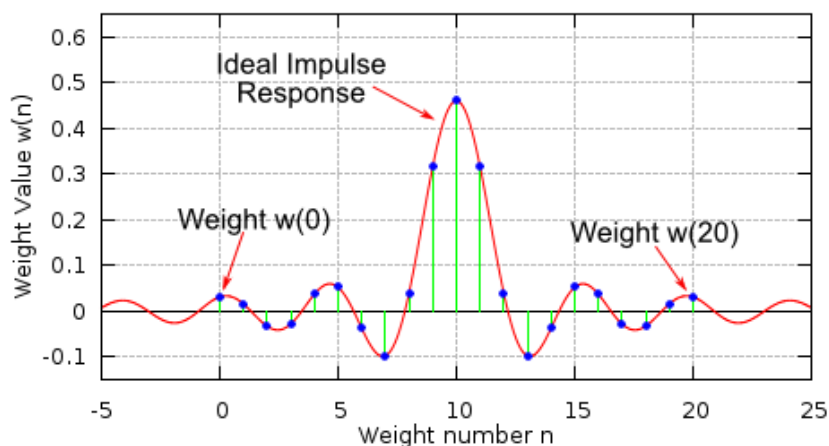


Figure 15: Filter weights $M=20$, $f_t=0.23$ [9]

By using following formulas, all the weights from 0 to 20 can be easily calculated. With those the filter can be implemented.

$$M = \text{filter length} - 1 = 20$$

$$f_t = \frac{\text{Cut off frequency}}{\text{Sampling Frequency}} = \frac{460}{2000} = 0.23$$

$$w_{lpf}(n) = \begin{cases} \frac{\sin[2\pi f_t(n - \frac{M}{2})]}{\pi(n - \frac{M}{2})} & n \neq \frac{M}{2} \\ 2f_t & n = \frac{M}{2} \end{cases}$$

Figure 16: Formulas to calculate the filter weights [9]

The figure below shows the frequency response of the real FIR LPF filter with a rectangular window [9].

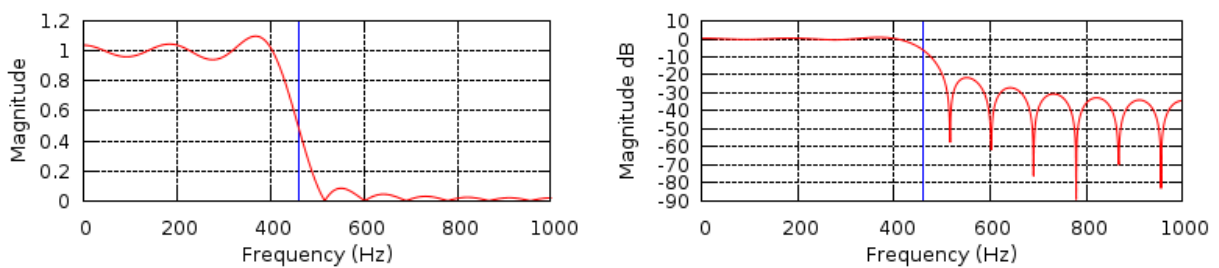


Figure 17: Frequency response of a real LPF using a rectangular window [9]

By applying different windows to the sinc functions, the performance can be increased furthermore. Following figure compares the Hamming window with the normal rectangular window. A performance improvement is clearly visible.

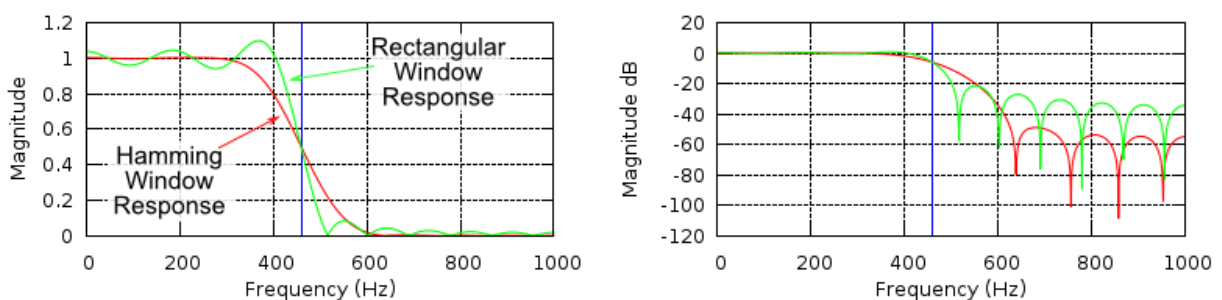


Figure 18: Comparison of Hamming window and rectangular window [9]

The implemented channel filter is a band pass filter, not a low pass filter. But such a band pass can be easily built by using the same principle like for the low pass. To get

a high pass filter you just have to subtract a low pass filter from an all pass filter. Afterwards one just has to combine the LPF and the HPF to get a band pass filter.

As the implemented channel filter is configurable, following table shows the sample rate reduction factor and the maximum allowed chip rate with regards to the channel filter setting.

Table 1: Channel filter selection

RED_SEL...Channel filter selection

CFBW...Channel filter bandwidth (bandpass filter, 99 % power bandwidth) in kHz

3dB BW...Channel filter bandwidth (bandpass filter, 3 dB bandwidth) in kHz

RCF...Sample rate reduction factor

MCR...Maximum allowed chip rate in kHz

CFG...Channel filter gain

RED_SEL	CFBW	3dB BW	RCF	MCR	CFG
0	600	700	1	200	1.00
1	300	350	2	112.5	1.00
2	200	233	3	75	0.84
3	150	175	4	56.25	1.00
4	120	140	5	45	0.98
5	100	117	6	37.5	0.84
6	75	87.5	8	28.13	1.00
7	50	58.3	12	18.75	0.84
8	37.5	43.8	16	14.06	1.00
9	25	29.2	24	9.38	0.84
10	18.75	21.9	32	7.03	1.00
11	12.5	14.6	48	4.69	0.84
12	9.38	10.9	64	3.52	1.00

2.3.3 Demodulator

Demodulation is performed by coordinate transformation from the complex I and Q signals to real amplitude and phase. The amplitude information corresponds to the received signal strength interface (RSSI) information and it is required for ASK demodulation. The phase output is fed into a FSK demodulation PLL.

A phase locked loop (PLL) is suited very well to demodulate a FSK signal. Generally, a phase-locked loop is a control system that tracks the frequency and phase of an input signal. Thus, the PLL is widely used in many types of analog telecommunication systems, such as an AM demodulator, FM demodulator, frequency selector, etc.

Similarly, a lot of digital phase-locked loops have been developed, e.g. to track a carrier or synchronizing a bit signal in digital communication systems [10].

Basically a PLL consist out of three major parts: Phase Detector (PD), Loop Filter (LF), and Voltage Controlled Oscillator (VCO). Following figure provides the block diagram of a PLL [10].

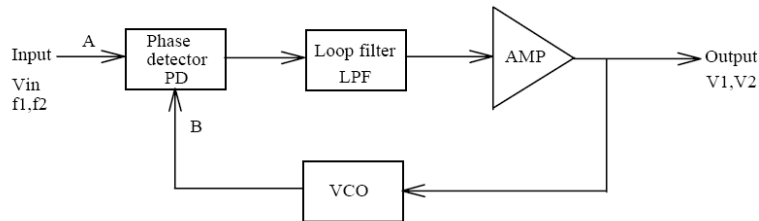


Figure 19 : BLock Diagram of a FSK Demodulation PLL [1]

Consider the PLL block diagram shown in the figure above. If the frequency of V_{in} changes, a rapid change will result in a phase difference between A and B and hence a DC level change at the output of the phase detector. This level shift will change the frequency of the VCO to maintain in the locked state. If a FSK signal is applied to the input of the PLL and if the PLL is used as an FSK demodulator, the output voltages V_1 and V_2 will correspond to the input frequencies f_1 and f_2 respectively. Thus an input frequency change is converted into an output dc level change. To finally get the FSK demodulated signal, a comparator having a reference between V_1 and V_2 must be connected to the output of the PLL. Its output will be a digital signal that can be used for further processing [10].

Before the signal can be fed into the clock data recovery its sample rate must be adapted so that it is between 16 and 32 samples per chip. A configurable decimation stage is provided for this task. The subsequent data filter (baseband filter) is a low-pass filter with a corner frequency of $1/16$ of the sample rate; i.e. the corner frequency is automatically adjusted when the correct oversampling rate is selected.

2.3.4 Clock data recovery

The clock and data recovery employs a matched filter as data filter. The data filter is matched to the expected signal waveform and it consists of two antipodal boxcar filters with the selected chip rate.

A matched filter (originally known as a North filter [11]) is mainly used in signal processing technologies. It is obtained by correlating a known signal, or template, with an unknown signal to detect the presence of the template in the unknown signal. This technique is equivalent to the convolution of the unknown signal with a conjugated time-reversed version of the known signal. The matched filter is perfectly suited for maximizing the signal to noise ratio (SNR) in the presence of additive stochastic noise [12].

Considering a transmitter sends the sequence "0101100100" coded in non polar Non-return-to-zero (NRZ) through a noisy channel. The original signal without any noise looks like in the figure below.

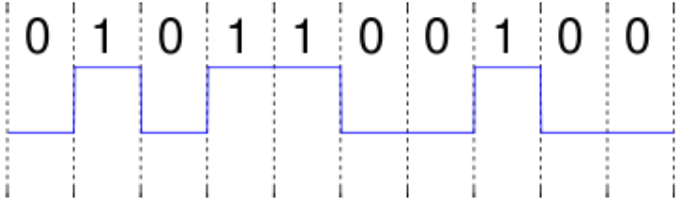


Figure 20: Transmitted data without additive white Gaussian noise [12]

If the channel is modeled as an AWGN channel, white Gaussian noise is added to the signal. At the receiver side, for a SNR of 3dB, this may look like the signal in the next figure.

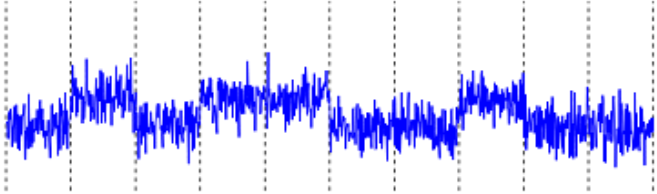


Figure 21: Received data with additive white Gaussian noise [12]

Without any tricks, we cannot reveal the original transmitted sequence. The power of noise relative to the power of the desired signal is very high, i.e. the signal-to-noise ratio is very low. To increase the SNR, the received signal is passed through a matched filter. The filter is matched to a NRZ pulse, precisely the impulse response of the ideal matched filter should be a time-reversed complex-conjugated scaled

version of the signal we are looking for. After convolving the noisy input signal with the matched filter, the signal looks like shown in the figure below.

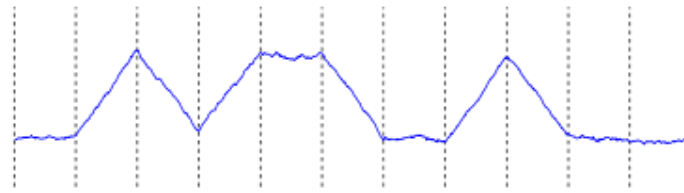


Figure 22: Received data after the matched filter [12]

This signal can now be sampled by the receiver at the correct sampling points, and compared to an appropriate threshold, resulting in a correct interpretation of the binary message. Following figure shows how the sampling could look like.

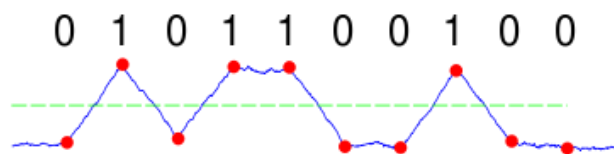


Figure 23: Sample points on the received signal [12]

It is important to note that the implemented matched filter is matched to the incoming data stream and not to the signal waveform. Therefore, the system is able to detect signals with different shaping waveforms (e.g. rectangular shaped or Gaussian shaped input signals with different BT values). Following block diagram shows the clock data recovery section of the implemented receiver.

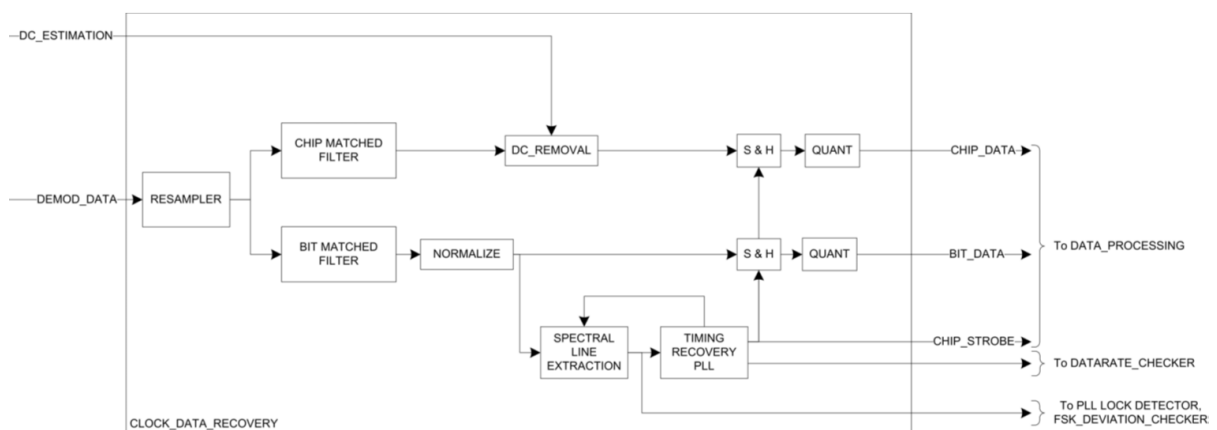


Figure 24: Block diagram of the clock data recovery [1]

The clock recovery consists of a fractional resampler stage which samples the incoming data at a 16 x chip-oversampled nominal data rate. This ensures highest sensitivity and best acquisition time also in presence of jammers and unwanted signals. This input stream is filtered by a chip- and a bit-matched filter in order to achieve data rate selective filtering. Using Manchester encoding, one bit is split into two chips, therefore the bit matched filter always uses the information of two chips to decode one bit of data. For the timing recovery, only the DC free bit matched filter output is to be considered as it gives the best signal to noise performance. To ensure the locking behavior of the timing recovery PLL, a static normalization stage levels the output of the matched filter such that the PLL has input signals with constant peak amplitudes. To improve the timing recovery, the chip rate is extracted from the incoming data stream at the spectral line extraction unit together with time timing recovery PLL.

The timing recovery PLL derives the chip clock out of the received data stream. The chip clock is used to sample the bit matched filter output as well as the chip matched filter output at the time instance where the signal power in the two filter outputs is maximized.

The output of the chip matched filter is not DC free and contains in FSK the frequency offset and in ASK a signal power dependent value. This DC component is unwanted and is removed in the DC removal stage.

Finally the sampled values are quantized at the output stage to provide binary (0, 1) data to the succeeding processing stages.

2.3.5 Data processing

The data processing block combines the functions of data recognition and packet building for valid data sequences and accommodates the transfer to the memory of the receiver. There are many functional blocks working together to carry out this functionality. The core functionality is covered by the receiver finite state machine (FSM).

The receiver state machine controls the high level reception states of the UHF receiver like wake up search, frame synchronization or data reception. The receiver supports the following major receive states:

State	Description	Criteria for proceeding	Criteria for exit
IDLE	The idle state is the reset state where the receiver is turned off.	CPU write	
WUPS	This state is intended to search for a wake-up signal based on certain signal properties or a certain bit pattern.	Wake-up found	Wake-up search failed
FSYNC	This state is intended to search for a specific frame synchronization pattern, which is used to distinguish the header of the telegram from the actual payload. Once the frame synchronization pattern is found, the receiver switches to DATA state.	Frame synchronization found	Frame synchronization failed
DATA	This state is intended to receive the actual payload.	End of frame detected	

The data processing provides two equal pattern matching units to the user. The pattern matching unit is intended for frame synchronization or wake up pattern search with a dedicated pattern. It consists of a shift register and two independent pattern compare units. This allows e.g. that pattern matching unit 1 is configured with bit data for wake up search, and pattern matching unit 2 with chip data for frame synchronization. These units are intended to be the main criteria for state transitions of the receiver state machine.

If the receiver state machine is in the DATA state, the actual payload is decoded and recorded. The user has the possibility to configure a direct memory access (DMA) interface in a way that the payload is stored at a certain memory position in the RAM. This interface is used to read out the received data in order to compare the payload to the transmitted data. For debug reasons or for communication with extern devices (e.g. μC), the selected data and clock can additionally be output at general purpose I/O ports.

2.4 Micro controller MRK3

This section provides an overview of the implemented microcontroller, type "MRK3". It is the latest processor type from NXP. Furthermore this section explains how the communication between the tool TestStation and the IC works.

2.4.1 Functional description

The MRK3 CPU (Central Processing Unit) uses a Harvard architecture with an 8/16bit ALU (Arithmetic Logic Unit). The instruction set supports 8-bit and 16-bit operations and is optimized for ASM and C programming. Due to an effective two-stage pipeline with separate data collection and execution unit, most instructions execute in a single clock cycle.

The CPU can access 64 kilobytes linear data address space and 64 kilowords linear code address space. Numerous addressing options allow effective code generation with high density. Furthermore, the CPU has a system / user mode flag which offers a direct 2-level security scheme. Moreover, the CPU contains an interrupt unit that can handle up to 16 different interrupt levels. The figure below shows the block diagram of the MRK3 CPU.

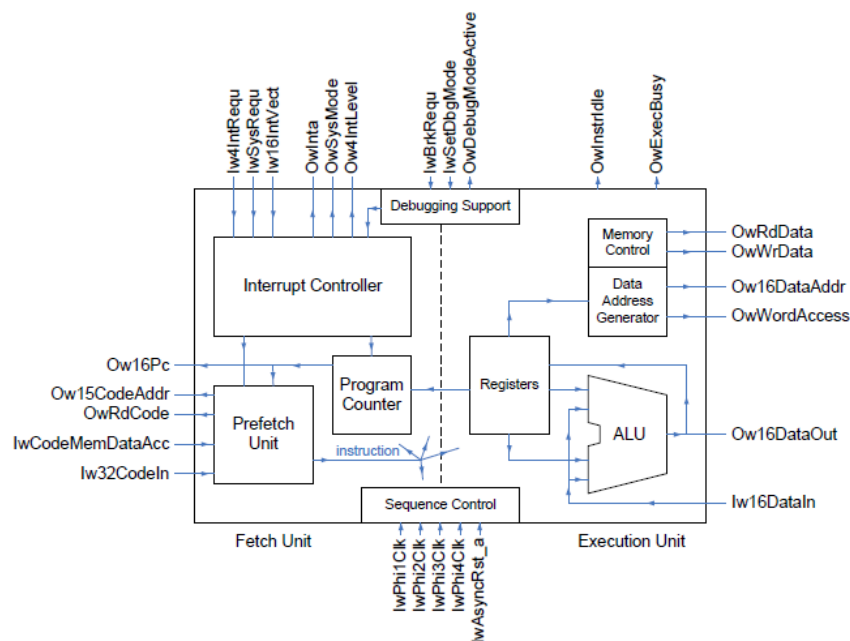


Figure 25: Block diagram of the MRK3 CPU [1]

Roughly speaking, the MRK3 architecture consists of two pipeline units. The fetch unit and the execution unit. The task of the fetch unit is to ensure the correct program flow, which is why it also contains the program counter and the interrupt controller. Furthermore it fetches the collection of code words from the code memory and provides a sequence of executable instructions to the execution unit.

The execution unit performs the data manipulation in the CPU. It calculates data addresses for memory instructions read operands from registers and / or from the memory, executes the requested command, writes the result of the operation back into a register or in the memory and updates, if necessary, the status flags.

2.4.2 Monitor and download interface

The communication between the micro controller of NXP's modern ICs and the TestStation is done via a communication protocol called monitor and download interface (MDI). This protocol is NXP self-made and implemented in the ROM code of the ICs. The interface is a two-wire serial synchronous interface consisting of two pins: MSDA (data) and MSCL (clock)

The MSCL pin provides the bit clock and is always driven by the chip. As long as the chip is in the reset state, the MSCL remains low. When the chip gets active, it sets MSCL to high.

The MSDA pin is a bi-directional pin and receives / writes the data bits, depending on the direction of data. The default state is HIGH, thus the IC connects an internal pull up resistor to the pin, when it is in reset state.

Available debug functions of the monitor and download interface:

- Starting the user application in real time or single step mode
- Interrupt the user application
- Interrupt the user application using breakpoints
- Read / write CPU register contents
- Read / write RAM contents
- Read / write application code from / to the non-volatile memories
- Non-intrusive read the device status
- Protection of the application code and application data

The figure below illustrates a typical MDI command including an answer of the device. The clock is always provided by the device, thus the IC is the clock master. Once the MSDA is pulled low from an external device, the clock for one command will be generated. After a short break the response of the device is read back, starting again with a negative edge on MSDA.

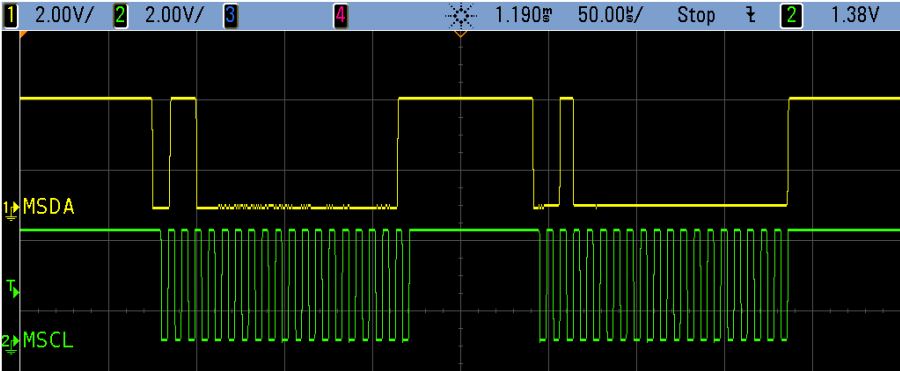


Figure 26: Illustration of a typical MDI command including a response of the IC

3. Measurement procedures and standards

This chapter describes the measurement procedures to be carried out on the automated test bench in detail. Also the engineer standards defining the measurements as well as the limits will be documented. Following table lists all the use cases that should be tested. All the measurement procedures listed below shall be carried out on each of these use cases.

Table 2 : Use case overview

Use Case ID	Modulation Type	Chip Rate tolerance	Chip Rate [chips/sec]	FSK deviation tolerance	FSK deviation [Hz]	CF-BW [kHz]
599	FSK	1%	1200	5%	1200	9,375
600	FSK	1%	2400	5%	2400	18,750
601	FSK	1%	4800	5%	4800	50,000
602	FSK	1%	9600	5%	9600	50,000
603	FSK	1%	9600	5%	35000	300,000
604	FSK	1%	50000	5%	50000	150,000
605	FSK	1%	100000	5%	100000	300,000
606	FSK	1%	2400	5%	2400	25,000
607	FSK	1%	15625	5%	15625	100,000
616	FSK	1%	15625	5%	20000	100,000
619	FSK	1%	100000	5%	50000	300,000
620	FSK	5%	10000	20%	20000	100,000
621	FSK	1%	40000	5%	20000	120,000
622	FSK	1%	1000	5%	25000	50,000
623	FSK	1%	1000	5%	25000	600,000
624	FSK	1%	8000	5%	200000	600,000
625	FSK	1%	200000	5%	50000	600,000
626	FSK	1%	200000	5%	200000	600,000
627	FSK	1%	1000	5%	500	100,000
628	FSK	1%	1000	5%	250	50,000
629	FSK	1%	38400	5%	20000	120,000
630	FSK	10%	19200	43%	35000	300,000
631	FSK	10%	19200	50%	20000	300,000
632	FSK	5%	38400	33%	30000	300,000
633	FSK	1%	2000	33%	30000	100,000
634	FSK	1%	11520	9%	5500	50,000
635	FSK	5%	16000	20%	8000	75,000
700	ASK	10%	1200	0%	0	9,375
701	ASK	10%	2400	0%	0	18,750
702	ASK	10%	4800	0%	0	50,000
703	ASK	10%	9600	0%	0	50,000
704	ASK	10%	8400	0%	0	300,000
705	ASK	10%	3400	0%	0	120,000
706	ASK	10%	1200	0%	0	300,000
707	ASK	10%	100000	0%	0	300,000
708	ASK	10%	19200	0%	0	300,000
709	ASK	10%	38400	0%	0	300,000

3.1 Receiver sensitivity

The receiver sensitivity is the minimum level of signal (electromotive force (emf)) at the receiver input, produced by a carrier at the nominal frequency of the receiver, modulated with the normal test signal modulation, which produces one of the general performance criteria stated below [14].

For the purpose of the receiver performance tests, the receiver shall produce an appropriate output after modulation under normal conditions as indicated below.

- a data signal with a bit error ratio of 10^{-2} without correction or
- a message acceptance ratio of 80 %

3.1.1 Method of measurement with continuous bit streams

In digital transmission, a bit error is a received bit extracted from a data stream, received over a communication channel that has been corrupted due to noise, interference, distortion or bit synchronization errors.

The bit error rate (BER) is the number of bit errors divided by the total number of transmitted bits during a certain time interval. BER is a unit less performance measure, often expressed as a percentage.

To perform such a test, a bit stream generator as well as a signal generator is necessary. The bit stream generator produces a pseudo random bit stream that is fed into the modulation input of the signal generator. The output of the signal generator is connected to the input of the receiver under test. The receiver is configured in a way, that it outputs the received data stream on IO ports to allow a comparison of the transmitted and the received bit stream. Following figure shows the block diagram of such a setup.

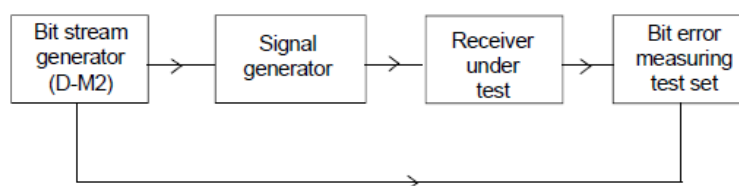


Figure 27: BER measurement setup

The bit stream of the modulated signal shall be compared to the bit stream obtained from the receiver output after demodulation. The level of the input signal to the receiver shall be reduced until the bit error rate is 10^{-3} or better. This input level is the sensitivity level, it shall be stored for post processing.

3.1.2 Method of measurement with messages

A message, also called a frame, consists out of three parts. The first part is the so called preamble, or run-in pattern. The purpose of this pattern is to wake up the receiver and train it before the next part of the message is transmitted. The receiver is now in the frame synchronization (FSYNC) state, in this state the receiver constantly demodulates the input data and searches for the frame synchronization pattern. On the transmitter side the preamble is followed by the synchronization pattern which will be detected by the receiver and interpreted as a state change to the DATA state. The last part of the message is the random payload which shall be decoded and stored by the receiver. The figure below illustrates how such a test message could look like.

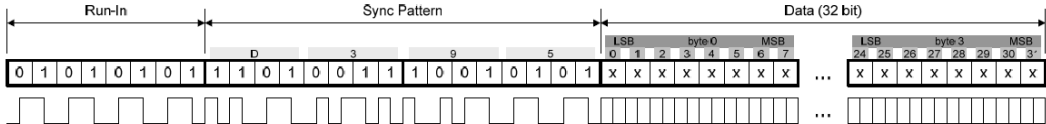


Figure 28: Test Message for FER Measurement

Following table shows the test messages that shall be tested in the automated test setup. For each of the test message types below, the sensitivity shall be measured.

Table 3: Message protocol overview

Frame ID	preamble	Synchronization pattern
0	10011001100110011001	1001100110011001
1	10100101	10010110
2	10100101	10101001
3	0101010101	010110
4	01010101010101	010101010101011110
5	000000000000111111111010101010	10101010101001
6	0101010101010101	1001011001100110

7	0101010110	01011001100110
8	0110011001100110	10100110010110101001011001100110
9	011001100110	0110000000001100110
10	110011001100110011001100	111000111000111000
11	101010101010	1111100110101
12	101010101010	11100010010
13	101010101010	10101010100101101001100110
14	101010101010	1010100101011001011001
15	01 01	101010101001011001011010

To perform such a test, a message generator as well as a signal generator is necessary. The message generator builds the test messages according to the table above and adds 4 bytes of pseudo random payload to them. These messages are fed into the modulation input of the signal generator. Between each message no signal must be sent in order to provide the same condition for every frame. The interframe time between two consecutive test messages is random, but must not exceed 100ms. The figure below illustrates how a random sequence of test messages could look like.



Figure 29: Timing of Test Message

The output of the signal generator is connected to the input of the receiver under test. The receiver is configured in a way, that it stores the received payloads in the device memory to allow a comparison of the transmitted and the received payloads. Following figure shows the block diagram of such a setup.

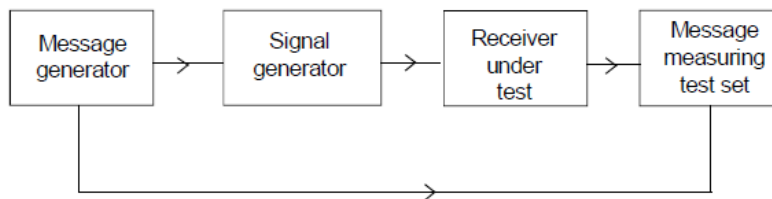


Figure 30: FER measurement setup

The transmitted payloads shall be compared to the payloads obtained from the receiver output after demodulation. The level of the input signal to the receiver shall

be reduced until the frame error rate is 10^{-2} or better. This input level is the sensitivity level, it shall be stored for post processing.

3.2 Receiver jammer performance

Beside the sensitivity of the receiver, the jammer performance is a very important parameter of the system. It must be guaranteed, that the receiver still operates with its full functionality, if an interferer is added on the wanted signal. Therefore three different interferer types are tested to ensure a proper functionality in the application. The jammer types are:

- CW: non modulated carrier
- AM: Amplitude modulation with 80% modulation depth and 200 Hz data rate
- FM: Frequency modulation with 20 kHz frequency deviation and 1250 Hz data rate

To perform such tests two signal generators A and B shall be connected to the receiver via a combining network. One shall transmit the wanted signal and the other one acts as the interferer. During the frame error rate measurement, the interferer is constantly on, only its level is modified. This ensures that the receiver experiences the maximum amount of stress, whereas the wanted signal is transmitted like described in the section “Receiver sensitivity”. Following figure shows a block diagram of such a hardware setup.

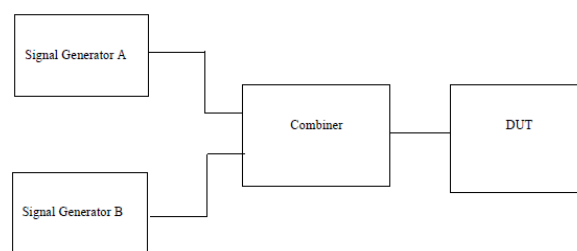


Figure 31 : Jammer measurement setup

In the first step, the modulated Signal is applied at receiver input without any interference and the sensitivity level is determined. Before switching on the interferer, an additional power of 3dB is added to the RX signal which is then held constant. The interferer is switched on the desired frequency offset, depending on the measurement procedure. Its power is raised until the reception of the wanted signal

shows a frame error rate of 10%. The difference between the receiver input level and the level of the interferer is called the isolation and is reported in decibel. Following figure illustrates the procedure.

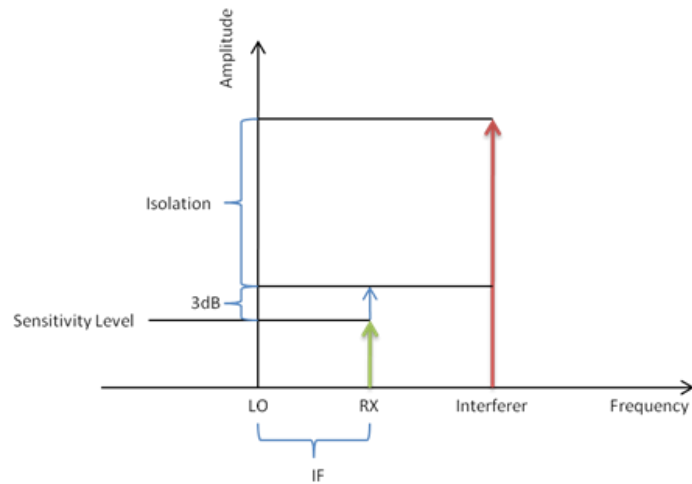


Figure 32: Principle of the interferer measurement

The following sections describe the different jammer positions and their purposes, these jammer measurements shall be carried out with all frames types using all use cases.

3.2.1 Adjacent channel rejection

Adjacent-channel interference (ACI) is caused by external power from a transmission in an adjacent channel. ACI may be caused by poor filtering, improper tuning or bad frequency control.

The adjacent channel selectivity is a measure of the capability of the receiver to operate satisfactorily in the presence of an unwanted signal, which differs in frequency from the wanted signal by an amount equal to the adjacent channel separation for which the equipment is intended [14].

The frequency offset for the adjacent channel is not fixed but channel filter bandwidth dependent. The next table shows the value for the first channel offset. The other jammer positions are multiple of the channel offset:

Table 4 : Channel separation for each channel filter bandwidth

Channel filter bandwidth	Adjacent channel separation
10 kHz	12.5 kHz
50 kHz	100 kHz
300 kHz	500 kHz
All other	Channel filter bandwidth + 25%

In total, six different adjacent channels shall be stressed. Three on the wanted band, and three on the image band. The figure below illustrates the jammer positions that shall be tested.

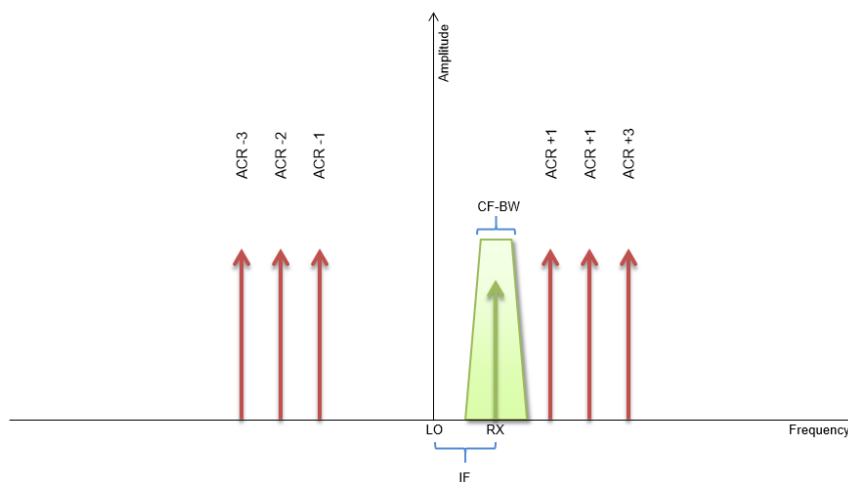


Figure 33: Position of ACR interferer

3.2.2 Co-channel rejection

Co-channel interference or CCI is crosstalk, caused by two different transmitters using the same frequency. There can be several causes of co-channel radio interference, the most probable reason is an overly-crowded radio spectrum of the band the receiver is used.

During the co channel measurement, the interferer is directly placed on the wanted signal. Thus, the interferer cannot be attenuated by the channel filter, which causes this jammer position to be the most sensitive one. Although the interferer is directly added on the wanted signal, the receiver should still be able to receive all of the transmitted messages until the interferer is about 10dB smaller than the wanted signal. Following figure illustrates the jammer position for this measurement.

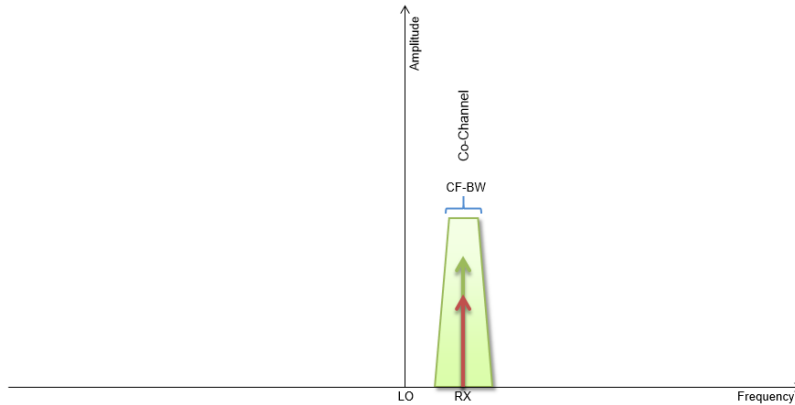


Figure 34: Position of Co-Channel interferer

3.2.3 Image rejection ratio

The image rejection ratio, or image frequency rejection ratio, is the ratio of the intermediate-frequency (IF) signal level provoked by the wanted frequency to that provoked by the image frequency. The image rejection ratio is usually expressed in decibel.

In a good design, ratios of >60 dB are achievable. Note that IRR is not meaningful for the performance of the IF stages or IF filtering, the signal yields a valid IF frequency. Rather, it is the measure of the IQ mismatch compensation unit described earlier in this study.

For this type of measurement, no interferer is needed. A sensitivity measurement is done on both, wanted and image frequency and the difference is the calculated image rejection ratio. Following figure illustrates this measurement.

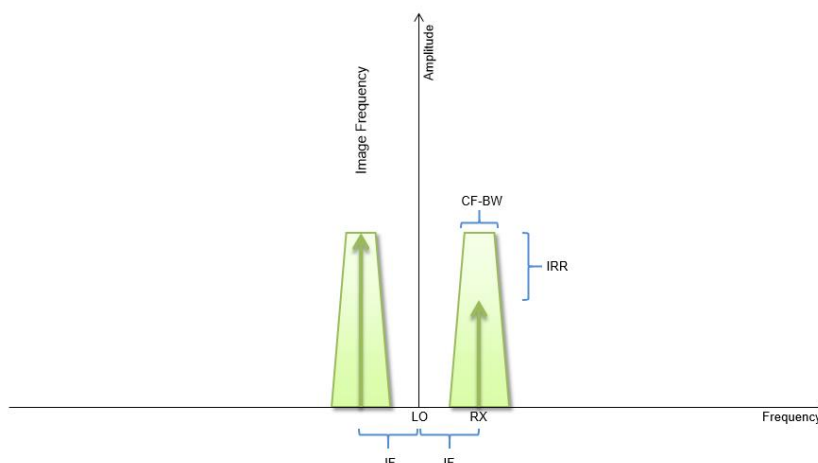


Figure 35: Illustration of the IRR measurement

3.2.4 Image channel rejection

During the image channel rejection measurement, the interferer is placed directly on the image frequency of the channel. This frequency is located at the receive frequency subtracted by two times the IF frequency. Due to the fact that an IQ mixer is used and furthermore an IQ mismatch compensation unit is implemented, the signal to jammer ratio should exceed the value of 50dB easily. Following figure shows the position of the image interferer.

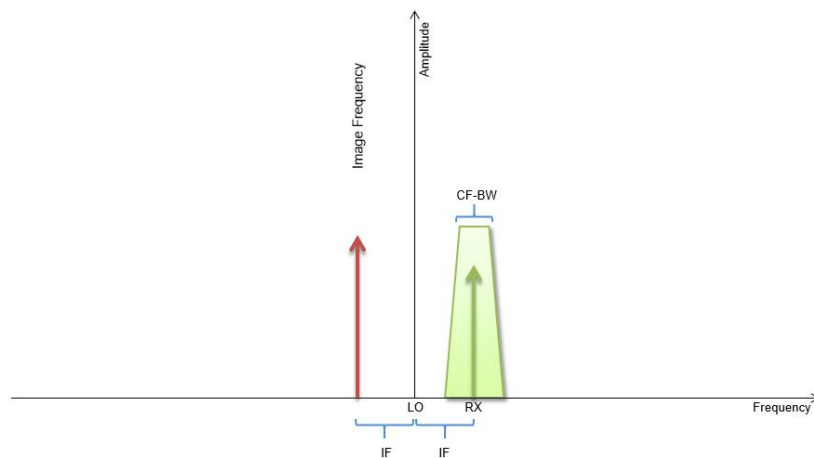


Figure 36: Position of the image interferer

3.2.5 Blocking

In radio, and wireless communications in general, blocking is a condition in a receiver in which an off-frequency signal (generally further off-frequency than the immediately adjacent channel) causes the signal of interest to be suppressed [15].

Blocking rejection is the ability of a receiver to tolerate an off-frequency signal and avoid blocking. A good automatic gain control design is part of achieving good blocking rejection [16].

Considering the definition above, this measurement procedure covers four different interferer positions, far away from the channel. It measures the capability of the receiver to receive the wanted signal without exceeding a FER of 10% during the presence of an unwanted input signal far away of the adjacent channels or bands. Following figure below shows the interferer positions to be tested.

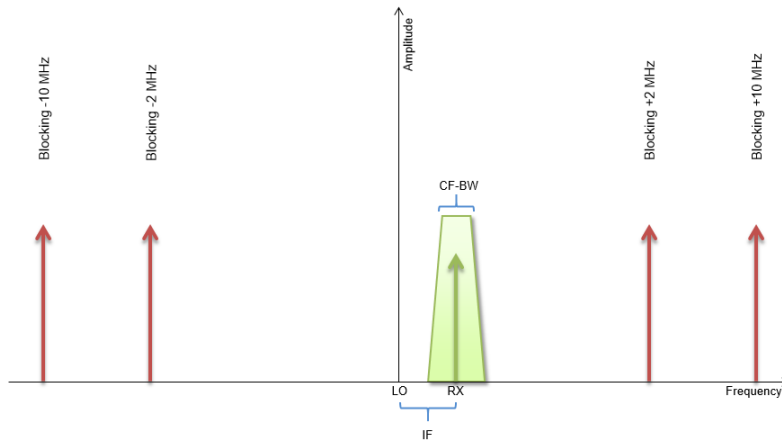


Figure 37: Position of the blocking interferer

3.2.5 Spurious response rejection

The spurious response rejection is a measure of the capability of the receiver to receive a wanted modulated signal without exceeding a given degradation due to the presence of an unwanted modulated signal at any other frequency, at which a response is obtained [14].

Furthermore, the ETSI standard says, that the limited frequency range where a spurious response could occur is defined as the frequency of the local oscillator signal applied to the mixer of the receiver plus or minus the intermediate frequency.

Considering the definition from the ETSI standard above, the measurement must be performed like the following: Like for all other jammer measurements, the wanted RX signal is kept constant 3dB above the sensitivity limit. The interferer frequency is swept over the whole frequency range indicated above. For each point, the signal to jammer ratio is measured, meaning that the jammer power is increased in every point as high, as the FER reaches 10%. This gives us a signal to jammer ratio (SJR) plot over the whole spurious response frequency area. Following figure shows, how such a measurement result shall look like. The zero point of the x-axis represents the RX frequency, the frequency plotted on the x-axis is the offset of the interferer to the RX frequency.

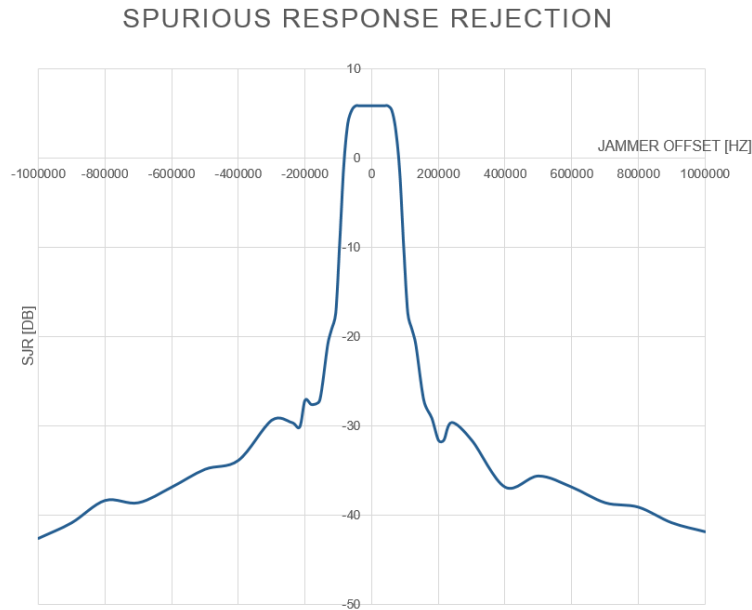


Figure 38: Illustration of a spurious response measurement

3.3 Modulation techniques

The receiver supports two different modulation techniques. Frequency shift keying (FSK) and amplitude shift keying (ASK). Both techniques are digital modulation schemes and base on the IQ modulation. Following chapters will explain them further.

3.3.1 Frequency Shift Keying (FSK)

Frequency shift keying is the most popular form of digital modulation. Its main application area is the short range communication like car fobs and similar systems. The simplest form of FSK is the binary FSK, where only two conditions (0 and 1) are defined. The digital baseband signal is modulated onto the carrier using a pair of discrete frequencies. With this scheme, the “1” is called the mark frequency and the “0” is called the space frequency. The difference between the space and mark frequency is called frequency shift, or frequency deviation [13].

Following figure shows, how a FSK signal looks like. It is shown in the base band, as a time continuous signal and also the unmodulated carrier is plotted.

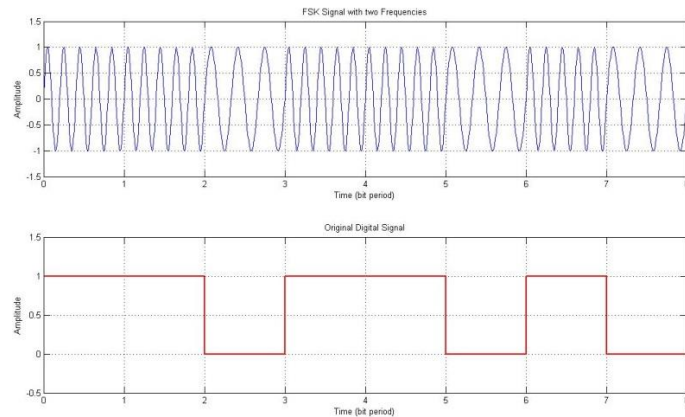


Figure 39 : FSK modulation principle [13]

3.3.2 Amplitude Shift Keying (ASK)

The amplitude shift keying is a form of digital modulation, where the baseband data is transmitted, by varying the amplitude of the carrier wave. If on-off-keying (OOK) is used, a binary “1” is represented by transmitting carrier wave of fixed amplitude and fixed frequency for the bit duration T . A binary “0” is represented by noise for the bit duration T . This makes it harder for the receiver to detect such a signal, because a binary “0” looks the same as “no signal”. Additionally it is sensitive to atmospheric noise, distortions, propagation conditions etc. Nevertheless it is used especially because of its low cost modulator and demodulator techniques. Following figure shows the principle of ASK modulation [13].

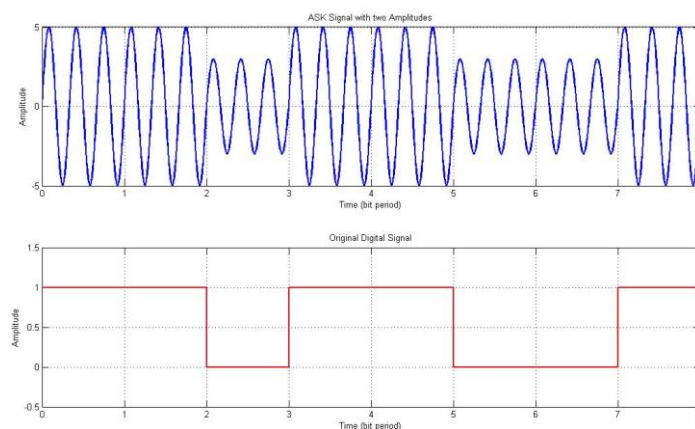


Figure 40: ASK modulation principle [13]

4. Implementation

In this chapter the final implementation will be presented. The first section will discuss the pros and cons of the verification using an FPGA and explains how such a FPGA can be used to fulfill the task of this study.

In the second section the hardware setup will be explained. Starting from a block diagram, every part of the setup, like the signal generator or the tool used for communication and modulation will be documented and discussed.

The implemented software is discussed in the third section. Not only one software was needed to get the system working, there are programs running on the micro controller of the front end IC, on the micro controller synthesized in the FPGA, on the communication and modulation box called "TestStation", as well as on the host computer.

4.1 FPGA - Field Programmable Gate Array

This section will answer all question regarding the keyword FPGA. It will explain what an FPGA is, how it can be used for this application and what limitations one has to cope with. Furthermore the strength and weaknesses of a verification using a FPGA will be discussed. One will experience, that such a verification has a lot more pros than cons, which is also the reason why this study gained a lot of interest within NXP Semiconductors.

A field-programmable gate array (FPGA) is an integrated circuit that can be configured by the end customer or a designer after manufacturing, that's why the name includes "field-programmable". The FPGA configuration is done via a hardware description language (HDL), like for all digital designs in an integrated circuit.

Modern FPGAs provide large numbers of logic gates and RAM blocks to enable the implementation of complex digital computations. FPGAs can be used to implement any logical function that an application-specific integrated circuit (ASIC) could perform. The ability to program the functionality after manufacturing, perform rapid prototyping of the design and the low engineering costs relative to an ASIC design, offer advantages for many applications.

4.1.1 Functional description

FPGAs contain configurable logic blocks, called CLBs or LABs, depending on the vendor. These CLBs are connected using configurable interconnects that allow the blocks to be wired together. This means, that many logic gates can be wired in many different configurations. Logic blocks can be configured to perform complex combinational functions, or as simple logic gates like AND or NOT. Most FPGAs also include memory elements like simple flip-flops or complete blocks of memory like RAMs [17].

Furthermore, input / output blocks (IO-blocks) are implemented on most of the modern FPGAs. They are used to communicate with the surrounding environment and are built to pass through the incoming signals to the configurable logic blocks. Also these blocks are configurable and can be suited to the application environment. For example, the output voltage as well as the input thresholds can be adapted to different standards like TTL or CMOS. Also driving strength and input impedance can be controlled.

To map an application circuit into a field programmable gate array, a FPGA with adequate resources must be chosen. While the number of CLBs and I/Os required for a design is easily determined, the number of routing tracks needed may vary considerably even among designs with the same amount of logic.

4.1.2 Hardware structure

A logic block (CLB) consists only of a few logical cells. A typical cell consists of a 4-input look up table (LUT), a full adder (FA) and a D-type flip-flop, as shown in the figure below. The LUTs in this figure are split into two 3-input LUTs, in the normal mode those are combined to a 4-input LUT. In arithmetic mode, their outputs are fed to the full adder. The mode selection is defined via the middle multiplexer. The output can be either synchronous or asynchronous, depending on the programming of the multiplexer to the right [17].

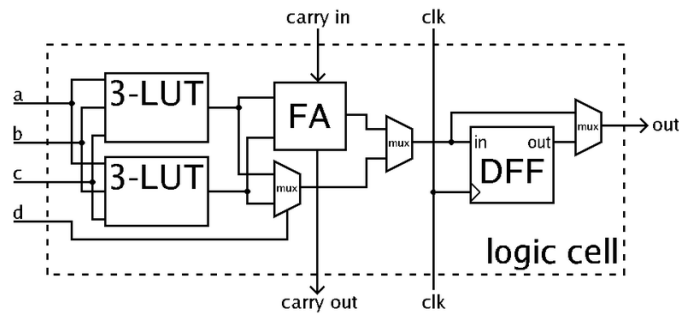


Figure 41: Block diagram of a configurable logic block [17]

Whenever a horizontal and a vertical channel intersect, there is a so called switch box integrated. One possible implementation of such a switchbox is, that a wire entering a switch box can be connected to one out of three other wires in adjacent channel segments. The figure below illustrates the connections in a switch box [18].

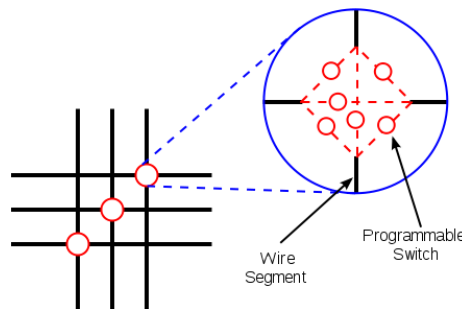


Figure 42: Connections in a switch box [18]

4.1.3 Design and synthesis

To configure the behavior of the FPGA, the user must use a hardware description language (HDL) to define the logic behavior of his design. The HDL is most of the times VHDL or Verilog, but also other languages are allowed. Once the code is finished, it can be used on any FPGA or even be used for an ASIC design.

Every vendor provides a tool, to convert the hardware description language into a so-called netlist, which is a list containing all the connection information of the used digital cells from the design. This procedure is called synthesis. This netlist isn't a well readable code anymore, but modern tools allow to look at the produced cells and their connection visually. The netlist can then be fitted to the actual FPGA architecture using a process called place-and-route, usually performed by the FPGA vendor's place-and-route software. For place and route a detailed description of the used hardware is necessary. This hardware description contains the number and

structure of the CLBs, the number and type of interconnects as well as the number of IO blocks. Once the process is complete, the binary file generated by the tool is used to configure the FPGA. This file is transferred to the FPGA via a serial interface (JTAG) or to an external memory device like an EEPROM [19].

4.1.4 Motivation for FPGA verification

The main verification solution is of course the digital simulation. Designing a test bench for a new digital block of the IC can require more working time than the design of the digital block itself. Nevertheless such a test bench is needed for every sub-block of the digital backend to prove its correct functionality. Therefore the digital design team introduced default use cases and a so called reference frame, which is an example of a modulated input signal fed into the digital receiver. All the simulations are done with this reference frame for all use cases. The simulation coverage is quite low if just one input frame and some chip rate / modulation index combinations are used. Unfortunately the simulation time is very high for such test benches, therefore the simulation coverage can't be increased easily. This limitation is also limiting the quality of the design itself, because a solid verification is the key to success in such design projects. Carrying out parts of the verification with a FPGA environment could increase the verification coverage enormously. More protocols and use cases could be tested and potential errors could be found faster.

One essential drawback of the digital simulation are the models of the transmitters and interferers as well as the models of the analog receiver frontend. All of the models are developed in computing tools like Matlab or similar and although they are fitting the real behavior very well, there is still a remaining uncertainty in terms of dynamic behavior etc. Therefore it is hard to determine if a simulation result is hundred percent representative for the final ASIC including the analog functionality. Choosing a FPGA verification is the best way to overcome this uncertainty, because real transmitters and the final analog front end are used to produce the input for the digital receiver chain.

Nowadays the time to market of an IC must be as short as possible, as the customer demand for new technology is constantly high. In a normal design process the customer has to wait with the implementation of his software and his use cases until

the first tested prototypes of the IC are available. This includes also the fab run which takes more than 6 weeks. If anything is delayed during the bring-up phase of the supplier (in this particular case NXP), this also shortens the remaining implementation time of the customer before the product is released. Providing a FPGA solution to the customer helps to overcome this delay. He can use the FPGA for the debugging of his software as well as for implementing his receiver use cases. When the first prototypes of the IC arrive at the customer, the same software without any modifications can be used. Also the configuration for the receiver are 100% compatible with the FPGA system.

4.1.5 Strengths

As the FPGA is re-configurable, potentially found errors can be fixed in the design and after a new run of synthesis and place and route the verification can continue. This way of working is called rapid prototyping, because errors can be found, fixed and verified very fast. If errors are found in the prototype on silicon base, a new fab run requires more than six weeks until the fixed version is available.

Once the FPGA system is up and running, more than one setup can run in parallel to produce even more output for the verification of the design. The number of simulations in parallel is limited by the amount of server computation capacity booked. Such computation capacity is very expensive, thus two or more FPGA setups in parallel are the cheapest solution to verify the design with a high test coverage.

As the test time of the FPGA system is very short compared to the simulation time, lots of use cases and protocols can be tested in a short time frame. Also the number of tested frames to distinguish the frame error rate can be quite high. In simulation this number has to be limited as it is crucial for the simulation time.

All of the firmware developed for the FPGA system can be reused without any modifications on the final IC. This is possible because the micro controller and its surrounding blocks like the memories are also synthesized in the FPGA. Therefore the software team can already debug their code before the prototype is available. This ensures a very short debugging time on the real IC.

One essential point to mention is, that the FPGA system already emulates the final IC. Therefore the test bench and its configurations can be fully reused for the verification of the silicon. The only thing that has to be updated, are the potential changes in the configuration of the analog front end compared to the one which was used for the FPGA verification. But except this small part, everything is plug and play when the prototype arrives. Therefore no double work is needed and the bring-up phase of the IC can be very short.

4.1.6 Weaknesses and limitations

To implement a digital design for the FPGA environment, some extra work of the digital design team is necessary. The whole implementation time could easily have a duration of more than one week, which is a lot in critical project phases. But it is worth to mention, that this implementation only has to be done once.

Of course cost is an important factor for the feasibility of the FPGA verification setup. Especially the signal generators needed for the bench are quite expensive. The FPGA board also costs in the range of a few thousand euros. Therefore not any number of setups can be built without exceeding the cost limit of the project.

None of the control signals that are routed from the analog part of the receiver are available in the FPGA application. The most important information that has to be passed to the digital part of the receiver are the ADC output signals (I and Q) as well as the ADC clock signal. Those can be multiplexed to a MFIO of the front end IC and thus passed to the MFIOs of the FPGA. The only control signal that cannot be forwarded, is the input for the AGC compensation unit. This units would scale the incoming data dependent from the attenuator settings at the frontend. In the FPGA implementation this compensation must be turned off.

Due to the fact that only one receive chain fits into the FPGA, parallel reception cannot be tested. In the final IC three receive chains are able to operate in parallel and decode signals from three different transmitters at the same time (considering the dynamic input range of the receiver).

One drawback of the FPGA verification is of course, that the exact timing behavior of the final IC cannot be modeled. Only the pure functionality can be tested. Thus, race

conditions, spikes as well as correct sample and hold times cannot be verified. This is also the reason why simulation will never be neglected in a professional verification strategy.

Additionally, the behavior over temperature and supply voltage also cannot be verified as the temperature behavior and the dependency on the supply voltage is mostly process dependent. The only thing that could be done, is to stress the analog frontend which produces the data for the digital receive chain. But as the FPGA test bench is built to test the digital functionality and not the analog one, such tests are not planned.

The prerequisite of such a FPGA based verification is of course, that the analog front end of the receiver to be verified is either already available on a test chip, or does not change tremendously compared to the previous version of the receiver. This is the case because a verification of the digital part of the receiver makes no sense, if the analog part (e.g. the Sigma Delta ADC) changes dramatically. Aim of the FPGA based verification is to test the whole system, frontend as well as backend.

4.1.7 Implementation effort

As the design was initially written to be embedded in an ASIC, there is some effort needed to make it synthesizable for a standalone FPGA application. The block which should be tested, the narrowband receive chain, will not work without its surrounding environment like the clock tree, the micro controller or the memories.

Therefore the digital design team developed a design which is suited for the usage on any FPGA, containing the most important functionalities of the ASIC including the micro controller, all memories, the main clock source as well as most of the IOs. Most important is of course the implementation of the digital receiver, but because of space limitations mentioned above, only one of the three receive chains is included.

Thus, a wrapper has been built around the top-level digital part of the IC, called `cai_mtc_i_fpga_top`. It implements clock and reset generation, the port logic and the page flash. The next figure shows the block diagram of this implementation.

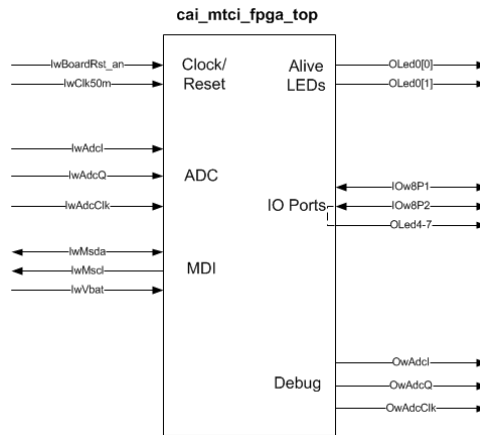


Figure 43: Block diagram of the FPGA implementation

The implementation uses the on-board 50 MHz oscillator as clock input, which feed directly into a PLL that produces various clock outputs:

- wClk82m: 82.8MHz
- wClk27m: 27.6 MHz master/system clock, XCLK
- wClk25m: 25.5 MHz (currently not used)
- wClk180k: 180 kHz low power RC clock

The internal reset is generated with the board reset input, the locked signal from the PLL and the input lwVbat, which is first synchronized and then fed into a 9 bit counter, producing approximately 1.5 ms delay on Vbat (see Figure below).

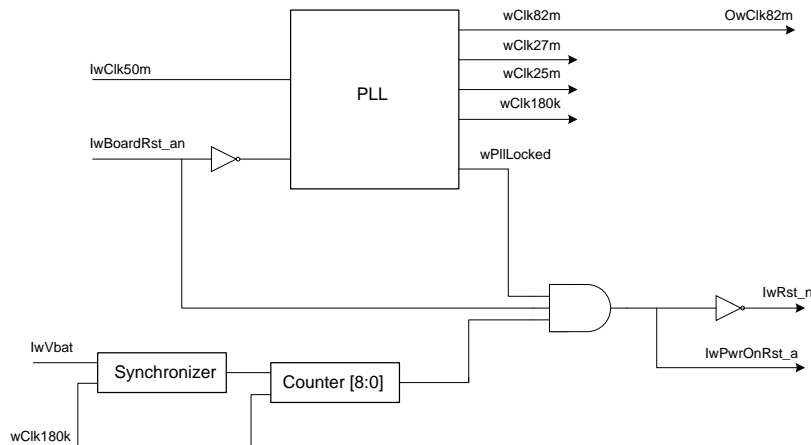


Figure 44: Clock and reset generation

Dependent on the selector input IxClk82mEn, either the external lwAdcClock or an internally generated 82 MHz clock is used as clock source for the digital top module (cai_mtc_i_dig_top). Therefore, SW0 has to be in ON position in order to operate the

design without external ADC interface over the daughter board. The clock and reset management unit within the instantiated digital top module is able to perform system clock switching between a derived version of this clock input and the generated wClk27.

Additionally, several system memory blocks have been replaced by dual-ported FPGA RAM resources, which can be read and modified during runtime with a so-called memory content editor. ROM and EROM are initialized with the resulting FPGA bit stream, while the RAM content is uninitialized.

Table 5 : Implemented memories

Component	Type	Size	Impl. Size	Instance ID
cai_kl_ram4k	RAM	4 KB	4 KB	RAM
cai_kl_rom16k	ROM	16 KB	16 KB	ROM
cai_kl_ram96k	RAM	96 KB	128 KB	RAMD
id_ee_pflashrlp32k_str	PFlash	32 KB	32 KB	EROM

It is important to note that the programming of the page flash memory is just emulated. Every write access goes directly into the internal RAM and not in a temporary buffer, since that would require lots of additional resources in the FPGA. However, an internal counter generates correct timing in case of erase and program operations. In order to implement an FPGA-ready bit stream the following tools are necessary:

Table 6: Necessary tools to implement a FPGA-ready bit stream

Task	Tool, Vendor	Vendor, Version
Synthesis	Synplify Pro, Synopsys	2010.09, Service Pack 3
Place & Route	Quartus II, Altera	10.1, Service Pack 1
Record/Playback Subsystem generation	SOPC Builder, Altera	Part of Quartus II installation

Based on the RTL code, the synthesis engine converts the design to a netlist, which is then translated to a gate level description. The second step is launching Quartus for doing the place and route of the previously generated netlist. Upon first implementation Quartus merges all the design units, initializes memories and implements the final bit stream (*.sof). Depending on the host machine and the constraints, this will last approximately 40 minutes.

4.2 Hardware setup

This section will describe the implemented hardware setup and all of its components in detail. The block diagram below illustrates which components are in use and how they are connected.

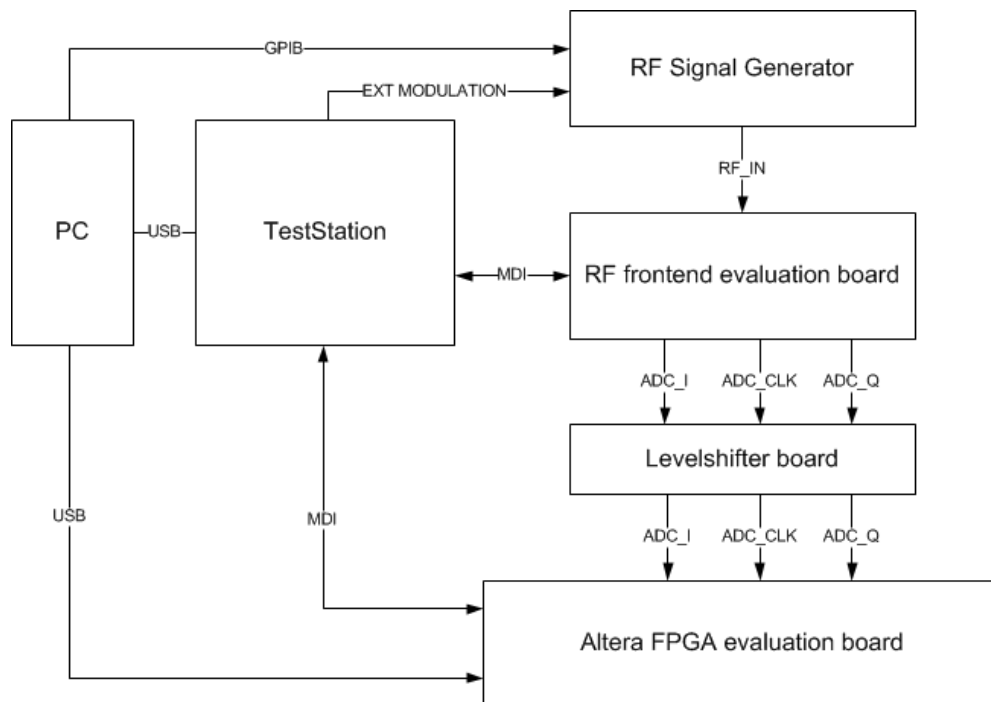


Figure 45: Block diagram of the hardware setup

The host of the setup is a personal computer (PC), it remote controls the signal generator as well as the tool TestStation which will be described below. Furthermore the PC is also used to download the configuration in the FPGA.

A very important part of the setup is the NXP self-made tool called TestStation. It is used to communicate with the RF frontend IC as well as with the IC synthesized in the FPGA. Furthermore it also forms the messages that are sent to the receiver. This is done by passing the base band data from the TestStation to the external modulation input of the signal generator.

The output of the signal generator is connected to evaluation board of the NXP frontend IC. The IC on this board is a predecessor of the product that shall be verified, whereas the analog part of the IC nearly remains unchanged. It is configured in a way that the ADC stream is outputted to IO ports, where the signal can be tapped and passed to the input of the FPGA.

The peak to peak voltage of the ADC stream outputted by the frontend IC is only in the range of 300mV. With such a small amplitude it is hard to be sampled by the input IOs of the FPGA, therefore a level shifter board is placed between the analog frontend and the FPGA evaluation board. It converts the 300mV peak-peak voltage to digital signal with an amplitude of about 3.3V using comparator circuits.

The FPGA is used in combination with an evaluation board provided by the company Altera. This board provides lots of connectors, buttons, LEDs, etc. to enable all of the features of the FPGA. Furthermore also an on-board 50 MHz oscillator is available which is used for internal clock generation. Beside a complete power management system with lots of available power supply outputs, this boards also contains a USB to JTAG interface, which enables easy programming via a personal computer.

4.2.1 Analog frontend

In order to use an already existing receiver type from NXP as an analog frontend, the RF evaluation board of the used IC is used. The evaluation board is seen in the figure below. The board provides the connectivity to all RF pins of the device as well as to the MFIO ports.

For the purpose of the FPGA test bench the receiver input is of course very important, thus the matching network that matches the receiver input to 50Ohm is necessary. On the used IC as well as on the evaluation board two different receiver input pins are available. Therefore two different matching networks for two different frequency bands can be used.

The communication interface MDI which is described in a different section of this study, is routed to a 5-Pin connector of the evaluation board. These pins must be connected to the communication tool TestStation.

The ADC interface pins, where the 300mV V_{pp} ADC Stream is outputted shall be connected to the input of the level shifter board. This can be done either with shielded cables or by stacking the evaluation board onto the level shifter board. To go for the second opportunity, one has to solder the connector on the bottom side of the board instead of original position on the front side.

The 3.3V supply voltage is available on the power supply of the FPGA evaluation board and can be taken from there.

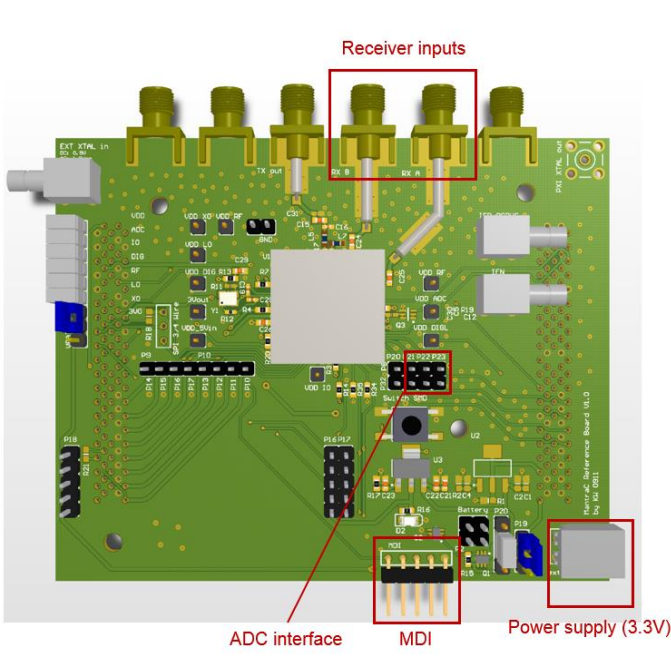


Figure 46 : RF frontend evaluation board

For details of the board, one can find the schematic of the RF frontend evaluation board can be found in the appendix A.

4.2.2 Level shifter board

The amplitude of the ADC stream outputted by the analog frontend is quite low. It is in the range of 300mV, which is far too less for a digital input to detect the threshold level correctly. Therefore a level shifter interface is needed between the analog frontend and the FPGA evaluation board. The schematic can be seen in the figure below. It consist of a voltage regulator, that converts the 5V board supply to a 3.3V supply, a voltage divider that produces the comparator threshold voltage of 100mV and three comparators that are supplied by the 3.3V and convert the 300mV ADC stream to a 3.3V digital signal. The 5V supply is available at the power supply of the FPGA evaluation board.

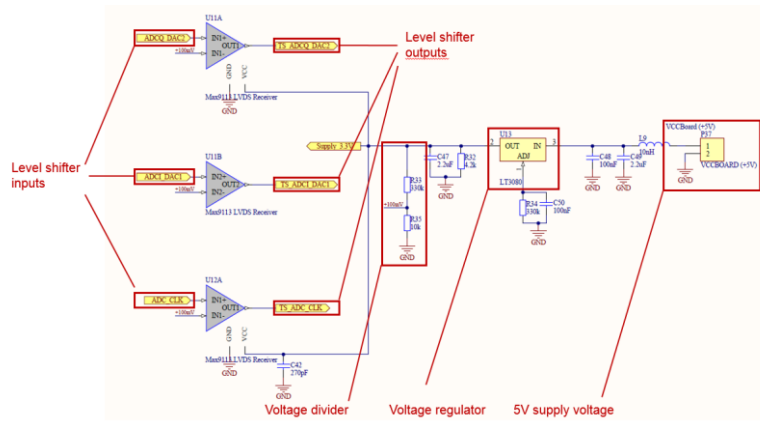


Figure 47: Schematic of the level shifter board

4.2.3 FPGA evaluation board

The Terasic DE3-150 board is used as prototyping hardware platform. It has populated an Altera Stratix III EP3SL150F1152C2N FPGA with approx. 142000 logic elements [20]. The board together with its interfaces is depicted in the figure below.

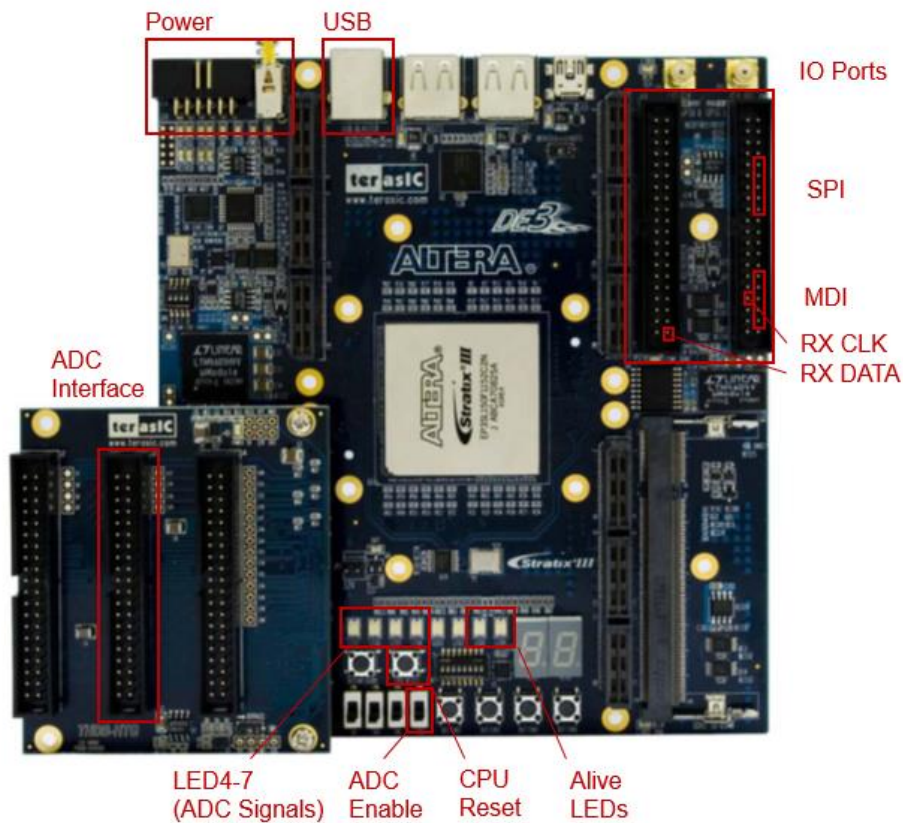


Figure 48: Terasic DE3-150 board

Following interfaces are implemented on the board:

- Power supply
- USB Blaster Download
- SPI interface
- MDI interface
- CPU reset button
- Port I/O (Button0 input, 4 LED outputs)
- Alive LEDs
- ADC interface
- ADC interface enable switch
- Debugging outputs

The level shifter board is placed directly on the ADC interface connector. The power cable is provided by the vendor and can be connected to a power supply which is also included in the package delivered by Altera. To connect the MDI interface, a small cable has to be built which can be connected to the communication tool TestStation. The SPI port as well as the debug outputs are not used at the moment. The detailed pinout can be found in the appendix B.

4.2.4 Signal generator

The FPGA verification setup needs a high performance signal generator with a very low phase noise and an operating frequency of at least 1 GHz. It must be able to perform FSK as well as ASK modulation, additionally there must be a possibility to feed the baseband signal into a device input for manual frame building. Furthermore it must be possible to turn the carrier signal on and off via an external signal fed into the signal generator. This function is needed to turn the carrier signal after the message immediately off.

The SMB100A signal generator from Rhode & Schwarz fulfills all these requirements and thus it was chosen to be used for the FPGA verification. Following figure shows the front panel of the device with all the most important interfaces highlighted [21].

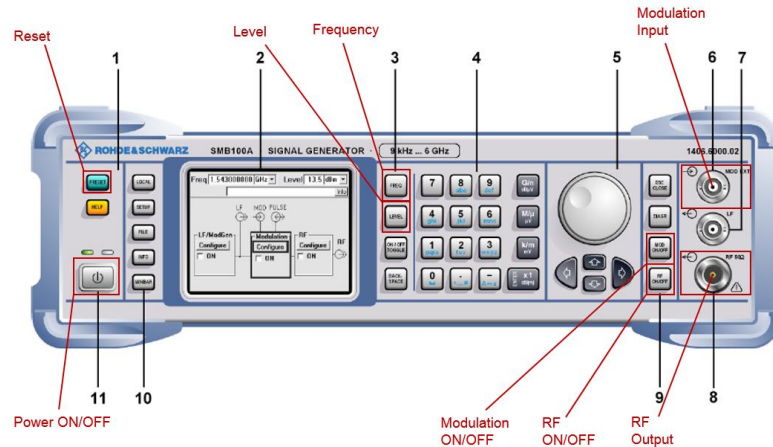


Figure 49: Front panel of the SMB100A signal generator [21]

After turning on the device via the power button, the first action is to press the reset button to start from a clean starting point. By clicking on the level and frequency buttons, the carrier parameters can be entered. After that, the wanted modulation must be configured in the menu. In the FPGA setup always two modulations are used concurrently: Either AM or FM modulation, and pulse modulation which is responsible for turning on the carrier before a frame and turning it off again once the frame is finished. It is important that the modulation source is configured as external, because the modulation input pin will be connected to the communication and modulation tool TestStation which is handling the frame building of the setup. By turning the modulation as well as the RF ON, the signal is outputted at the RF output connector which has to be connected to the RF frontend evaluation board.

Following figure shows the rear panel of the signal generator with all the most important interfaces highlighted [21].

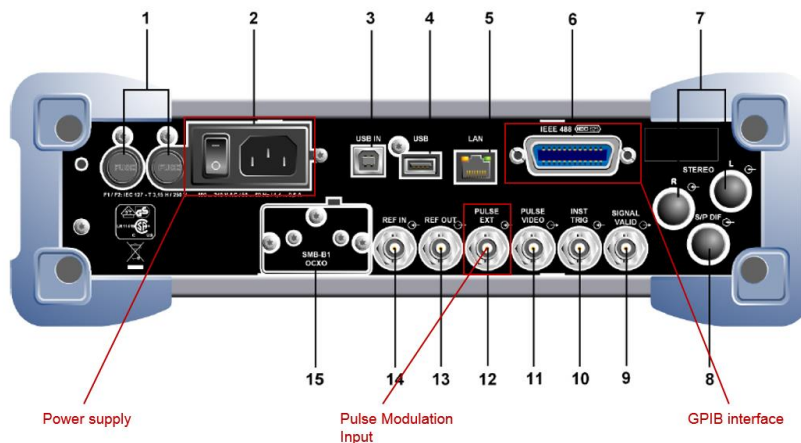


Figure 50: Rear panel of the SMB100A signal generator [21]

The power supply input must be connected to a 220V AC supply, and the power switch must be at the position ON. The pulse modulation input is used to turn the carrier on when the message begins and immediately off once the message was sent. This connector must be connected to the communication and modulation tool TestStation. It will control the message building of the FPGA setup. The GPIB interface is connected to the host computer. It is used to remote control the signal generator with the host software.

4.2.5 Communication and modulation tool “TestStation”

The TestStation is a NXP made tool, providing 28 mixed signal channels for arbitrary usage. Thus, it enables a way to contact all pins of an IC, force voltages and currents as well as measure voltage and current. It is also possible to communicate digitally over the channels and to manipulate the IO ports of the IC.

Originally it was developed for the "Complaint Handling" team to support the failure analysis of the customer returns. Today it is a broadly used solution, one can find it during the bring-up phase, in the characterization as well as in special purpose measurement setups like the one of this study. The figure below shows the front side view of the TestStation.



Figure 51 : NXP made tool “TestStation”

The block diagram below shows the basic structure of the TestStation. The communication with the host computer is done via the USB port. The USB port is connected to the DSP (Digital Signal Processor). This DSP controls the program flow and communicates with the TestStation software on the PC (personal computer). The

FPGA (field programmable gate array) is used for high-speed applications, however, it acts as a slave on the DSP.

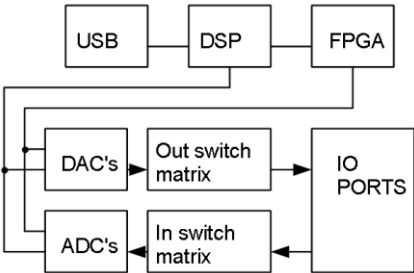


Figure 52: Block diagram of the TestStation hardware

The DSP and the FPGA both have full control of the ADC (Analog Digital Converter) and DAC (Digital Analog Converter) of the TestStation hardware. Depending on the required speed, either the DSP or the FPGA is used. These ADCs and DACs are connected to a switching matrix. This creates a very flexible way to connect the ADCs and DACs to all of the IO ports.

The TestStation has a plurality of DA converters (DA0 to DA9) which can be connected arbitrarily to all IO channels. All AD converters (AD0-AD10) can be connected either for voltage- or for current measurement to the IO channels. An overview is shown in the figure below.

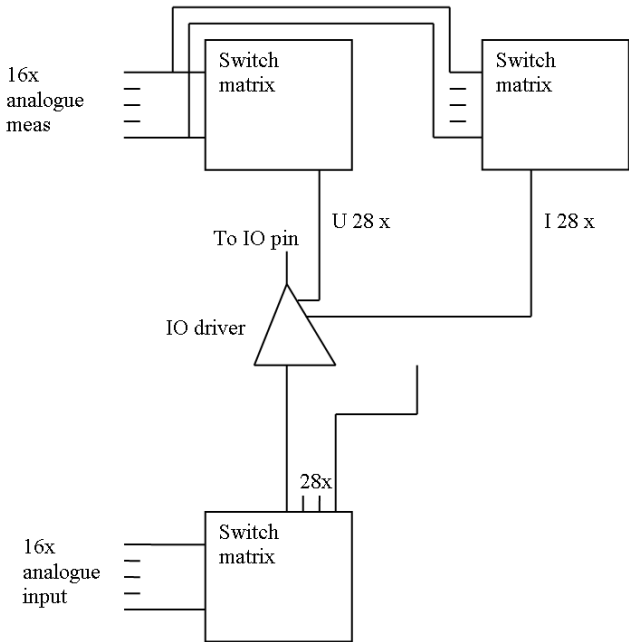


Figure 53: Internal structure of the TestStation

The comparator inputs for digital use are associated with DA3. The input threshold of the comparator is always DA3 divided by two. For example, if DA3 is set to 3 V, the threshold between LOW and HIGH is 1.5 V.

The TestStation has 28 channels (CH0 to CH27). The block diagram of each channel is shown below. The input may either be connected to GND, or to the analog input signal coming from the switching matrix. Each channel can provide and record current, the current is limited via switchable resistors. The current measurement resolution depends on this current limitation, since the current is measured as a voltage drop across this resistance. Furthermore, another switch for each channel is available, which connects the output driver with the channel or sets it to high impedance. The voltage measurement is always available, regardless of whether the driver is connected to the channel or not. The current measurement is of course only possible while the channel is connected to the driver. The following figure contains the block diagram of one TestStation channel.

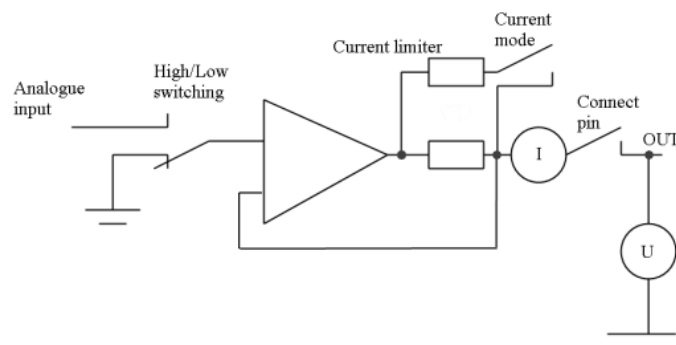


Figure 54: IO driver structure of the TestStation channels

4.3 Environmental software

This chapter will explain which software packages were implemented to get the FPGA verification test bench up and running. Totally there were three different software implementations necessary to build up the whole system. The most important part is running on the host PC of the setup which is the topic of the next chapter, it controls all hardware parts of the setup like the signal generator and the TestStation. Furthermore firmware updates for the TestStation and a firmware for the frontend IC were necessary, those are documented in this chapter.

4.3.1 TestStation firmware

The TestStation firmware consists of two parts, the DSP firmware and the FPGA firmware. Both parts will be explained in this section.

The DSP firmware has been developed in C++, it includes the communication with the host computer, the execution of commands, and the processing of interrupts. Once the firmware receives a command from the PC, it reads the command code as well as optional parameters, and jumps to the appropriate command routine. The execution of the commands happens sequentially, a parallel execution of commands is not possible.

For this study, two new commands have to be implemented in the DSP firmware. They are needed to use two TestStation channels as input for the modulation pins of the signal generator. One channel shall be used to enable/disable the RF output of the signal generator via the external pulse modulation input. The second channel shall be connected to the external modulation input of the signal generator and must therefore contain the digital baseband data that should be transmitted. The figure below illustrates how the output of the implemented commands looks like.

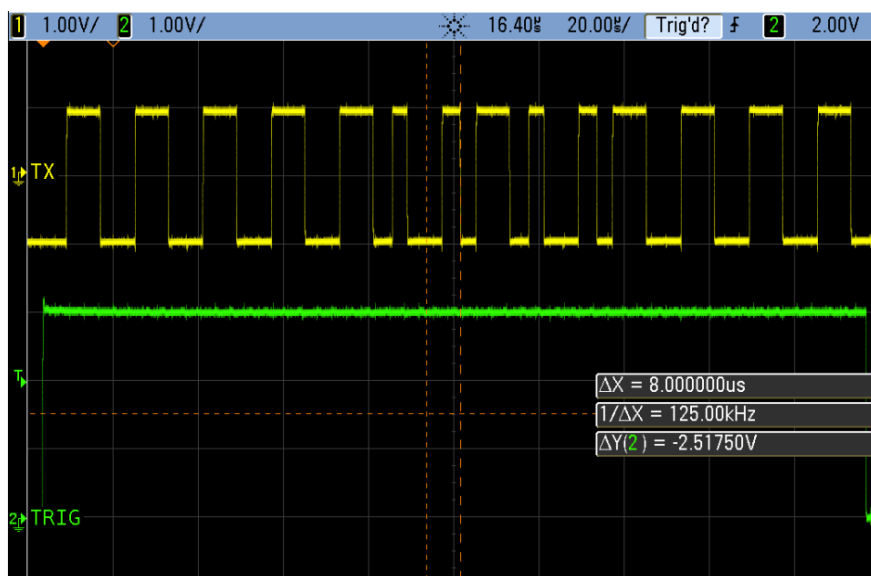


Figure 55: Illustration of the output of the implemented command

The first command is meant to be executed only once, it is the setup command and defines the channel numbers for the signal outputs as well as the chip rate and the logical high and low voltages. Following code snippet illustrates the command and its parameters.


```

/// <summary>
/// Setup the RF data frame sending system
/// </summary>
/// <param name="pinChannel">Pin at which data will be sent</param>
/// <param name="triggerChannel">Pin at which trigger will be sent</param>
/// <param name="bitTime">Time per bit in ns</param>
/// <param name="dataHighVoltage">Voltage of the dataline for high signal</param>
/// <param name="dataLowVoltage">Voltage of the dataline for low signal</param>
public SetupRFdataFrame(int pinChannel, int triggerChannel, int bitTime, double dataHighVoltage, double dataLowVoltage)

```

Figure 56: Command to setup the RF data frame system

The second command triggers the actual frame transmission. By executing the following command, including the parameters that define the length, the data as well as the encoding of the frame, the baseband data will be outputted on the channels defined with the first command.

```

/// <summary>
/// Sends a generic frame
/// </summary>
/// <param name="bitCnt">Number of bits to send</param>
/// <param name="data">Data</param>
/// <param name="isManchester">0 for NRZ encoding, 1 for Manchester encoding</param>
public SendGenericDataFrame(uint bitCnt, uint[] data, bool isManchester)

```

Figure 57: Command to trigger a frame transmission

The FPGA firmware is responsible for all high-speed applications over 1 MHz. It works as a slave of the DSP firmware, is thus controlled by the DSP. The FPGA firmware is in a stable condition and does not need to be changed for this project.

4.3.2 Host software environment

The TestStation Windows software is the heart of the project. Consisting of nine DLLs (direct link library), it is structured in two parts: In the restricted part which is intended only for TestStation developers, and in the public part for the engineers that are using the tool. The utilized development environment is Microsoft Visual Studio C # 2008 Express Edition with the .NET version 3.5.

The reason for this separation is, that the TestStation developers need to ensure that the communication with the TestStation firmware, with the laboratory equipment and the GUI (graphic user interface) works perfectly smooth. Furthermore all interfaces between these parts must be designed in a structural and clean way. Meanwhile, the TestStation users can create their own test cases without having to worry about the deep background of the software. They are only using simplified high-level functions to implement their tests cases.

A typical test case would setup certain TestStation channels properly (e.g. the supply of the IC), configure the MDI interface correctly (for example, turning on the receiver) and finally measure any voltages and currents (e.g. IBAT). The storage is also done automatically and can be exported via high-level commands to formats such as Excel.

One of the great strengths of the software, and the entire TestStation project is that it is compatible with almost any NXP product from the product line "Car Access and Immobilizers". Thus, a common test platform for all the products has been created.

The TestStation GUI already offers many pre-made functions such as reading and writing of special function registers, the up - and download of program code, and much more. The FPGA test bench is integrated in this GUI to provide a further extension for the TestStation users. Following figure shows the start window of the TestStation GUI.

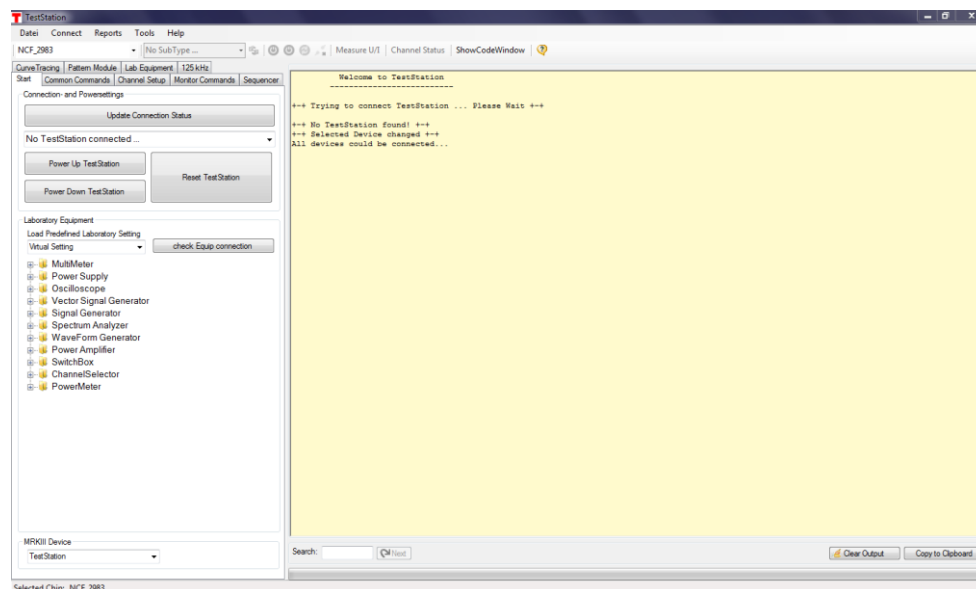


Figure 58: Start window of the TestStation GUI

4.3.3 Frontend IC firmware

As the frontend IC acts roughly speaking as a frequency down converter and as an analog to digital converter, the firmware running on the frontend micro controller has to fulfill two main operations.

The first task is to bias the analog cells that are needed for receiver operation, therefore more than one firmware is needed in order to have the possibility to receive

at different frequencies. There are three different versions available, one for 315 MHz, one for 434 MHz and one for 925 MHz, as these are the operating bands of the receiver. The only difference between these different firmware types, is the setup of the local oscillator which is the input of the IQ mixer.

The second small but very important segment is the output of the ADC stream to port pins. Three different port pins are necessary for this purpose: ADC_CLK, ADC_I and ADC_Q. The signals are switched out by a multiplexer that was implemented exactly for this purpose. This multiplexer is placed directly at the interface between the analog and the digital part of the receive chain.

The digital receive chain of the frontend IC is in idle state as only the receive chain of the newest prototype, synthesized in the FPGA shall be tested. Optionally, the receive chain of the frontend IC could also be activated for a direct comparison with the FPGA output.

After the necessary configuration, the micro controller of the frontend IC remains in the idle state as no further operation is necessary. All of the functionality runs autonomously without any interaction with the CPU.

4.3.4 Backend IC Firmware

For the first version of the FPGA verification setup no firmware for the micro controller synthesized in the FPGA is necessary. The whole digital receive chain runs autonomously without any interaction with the CPU needed. All the necessary operations are handled by the receiver state machine implemented in the digital receive chain.

4.4 Host software

This chapter will explain which software packages were implemented on the host computer to get the FPGA verification test bench up and running. The host software is the most important part of the setup, it controls all hardware parts of the setup like the signal generator and the TestStation and ensures the correct handling of the configuration files, the test case execution as well as the result file conversion. In this chapter all of the implemented functions and test cases are documented.

4.4.1 Frame error rate measurement

The measurement of the frame error rate (FER) is the core functionality of the FPGA based verification, all test cases are calling this function as it expresses the function of the receiver under the applied conditions. One frame is evaluated in several steps, the block diagram below illustrates the flow of this measurement.

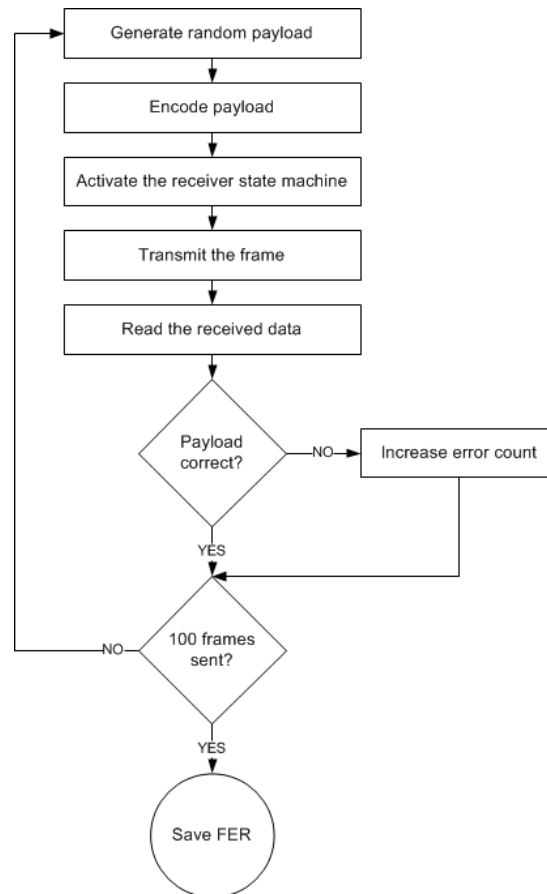


Figure 59: Block diagram of the frame error rate measurement

First the random payload is generated by a random number generator, followed by the encoding (NRZ or Manchester) of the data. Furthermore the preamble as well as the synchronization pattern depending on the frame type are added.

Once the frame is formed, the receiver state machine has to be set to frame synchronization mode. This is done via MDI communication over the TestStation. Afterwards the transmission can start, again this action is carried out by the TestStation which outputs the data on the modulation channels to the signal generator.

After the frame was sent, the received payload is read from the FPGA via the TestStation using again MDI communication. This action is followed by the comparison of the transmitted data and the read data. If the reception went wrong, the error count is increased.

After one hundred loops, meaning the transmission of one hundred frames, the error count represents the frame error rate in percent. This number is returned to the calling function.

4.4.2 Sensitivity measurement

The sensitivity measurement routine is a simple loop that starts with a quite high power level that the receiver should accept in any case and decreases the power level of the wanted signal as long as the frame error rate is less than ten percent. The block diagram below illustrates the rough functionality of this routine.

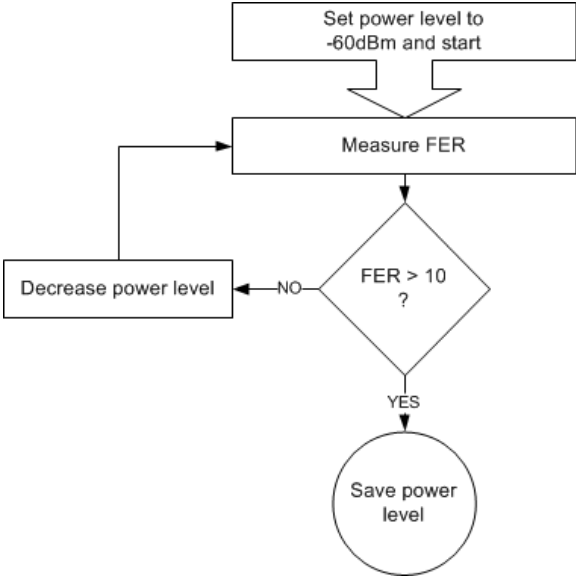


Figure 60: Block diagram of the sensitivity measurement

The routine has a binary search system implemented to decrease the measurement time. A linear search system would require much more time than this method. The output of the function is a power level in dBm which is returned to the calling function.

4.4.3 Sensitivity test case

By using the low level functions above, the top level sensitivity test case can be implemented. It uses a XML configuration file as its input and has to be carried out for all use cases. It contains several loops that are illustrated in the flow chart below.

After loading the configuration, the proper firmware (depending on the chosen RX frequency) is downloaded into the memory of the frontend IC. Once the firmware is started, the calibration of the RX frequency can be done. This is needed because the on-board crystal oscillator has a minor offset depending on the ambient temperature. This offset is at most 12ppm, but as this frequency is multiplied several times by the local oscillator, a final error of about 10 kHz can occur.

Once this is done, the signal generator can be set up depending on the selected use case. Afterwards two interleaved loops handle the proper program execution. The first loop iterates through NRZ and Manchester encoding, the second loop iterates through all available frame types.

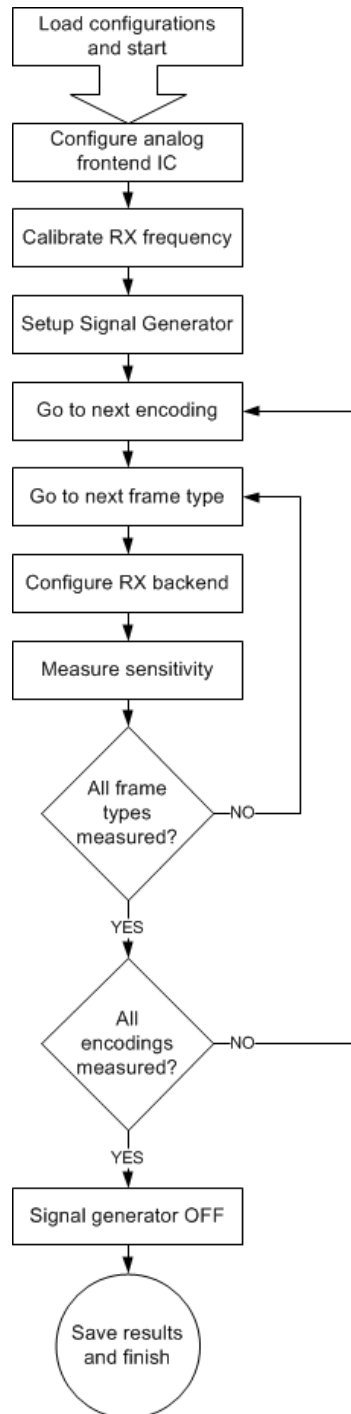


Figure 61: Flow chart of the sensitivity test case

Each loop iteration contains beside the sensitivity measurement, the configuration of the digital receive chain in the FPGA via the TestStation over MDI. This is needed because every frame type has its own configuration (e.g. the pattern matching unit for frame synchronization).

Once both loops are finished, the signal generator is turned off and the results are saved in a result file which can be converted to different output types later on.

4.4.4 Enhanced sensitivity test case implementation

The enhanced sensitivity test case uses the functionality of the default sensitivity test case and adds up one out of three possible additional loops. All other functionalities stay the same.

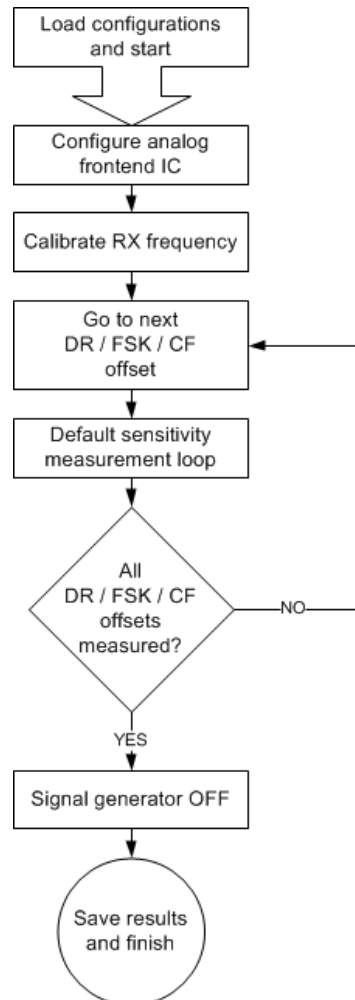


Figure 62: Flow chart of the enhanced sensitivity measurement

The first possible additional loop is the sweep over the data rate offset, simulating a transmitter that uses a not calibrated clock source. In low cost applications such transmitters are not seldom. The sweep is done in 1% steps from -10% of the nominal data rate to +10%.

Since the not calibrated reference clock source also influences the transmit frequency and the FSK deviation, the second and third loop opportunities are the sweeps over the center frequency offset and the FSK deviation offset. Again a sweep from -10% to +10% of the nominal value will be performed.

4.4.5 Signal to jammer ratio measurement

The signal to jammer ratio is calculated by the difference of the wanted signal power level and the jammer power level that causes a frame error rate of ten percent. Therefore the maximum jammer power must be found, where the frame error rate is still below ten percent.

The measurement routine is a simple loop that starts with a quite low jammer power level that the receiver should accept in any case and increases the level of the jammer as long as the frame error rate is less than ten percent. The block diagram below illustrates the rough functionality of this routine.

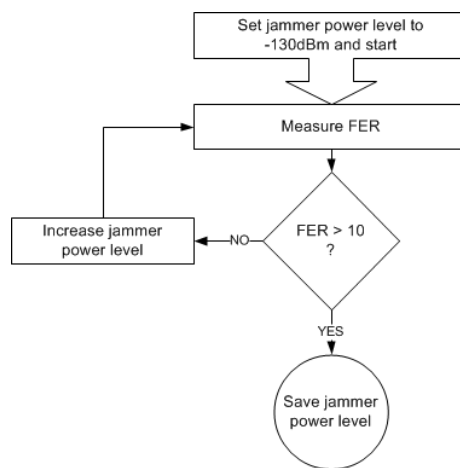


Figure 63: Block diagram of the signal to jammer ratio measurement

Also this routine has a binary search system for test time optimization implemented. A linear search system would require much more time than this method. The output of the function is a jammer power level in dBm which is returned to the calling function. The calling function will calculate the signal to jammer ratio using this value.

4.4.6 Interferer performance test case

By using the low level function above, the top level interferer performance test case can be implemented. It uses a XML configuration file as its input and has to be carried out for all use cases. It contains several loops that are illustrated in the flow chart below.

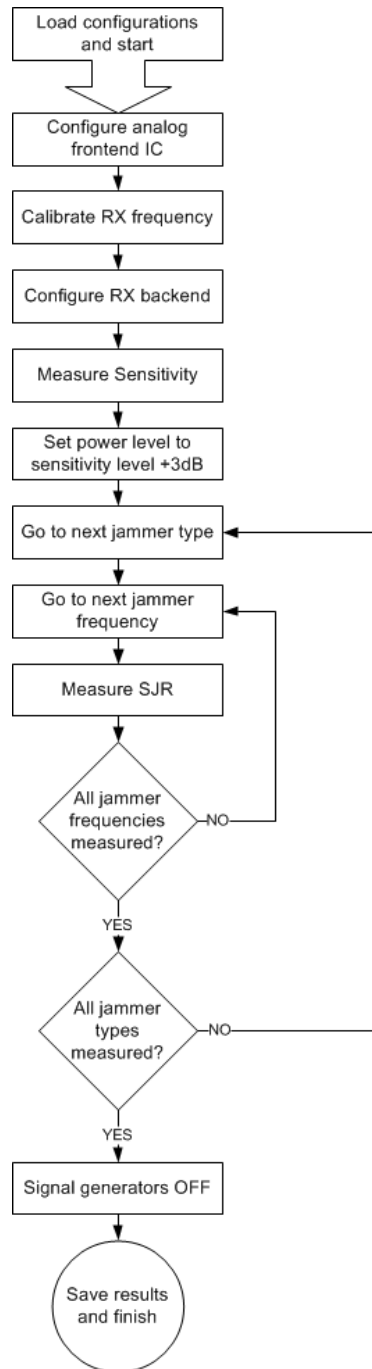


Figure 64: Flow chart of the interferer performance test case

Like for the sensitivity test case, the proper firmware is downloaded into the memory of the frontend IC. Once the firmware is started, the calibration of the RX frequency can be done. Once this is done, the sensitivity of this use case, using the reference protocol (frame ID 8) and Manchester encoding is measured. The wanted signal level is configured to the sensitivity level plus 3dB.

Two interleaved loops are handling the measurement of the signal to jammer ratio for all different jammer types and jammer frequency offsets found in the configuration

file. Once both loops are finished, the signal generators are turned off and the results are saved in a result file which can be converted to different output types later on.

In the last chapter of this study, one can find a section about possible measurement time optimizations using a firmware on the backend IC. For further details continue reading in that section of the study.

5. Results

This chapter shall present the results of this study, it will illustrate how the implemented setup looks like, which configuration files are available as well as how the result handling was done.

5.1 Hardware setup

This section will colorfully show, how the hardware setup was implemented. Two pictures show the core of the setup as well as a complete view of such a verification bench.

The graphic below shows the top view of the core of the FPGA verification setup. It contains of the Altera FPGA evaluation board and its power supply as well as the RF frontend evaluation board.

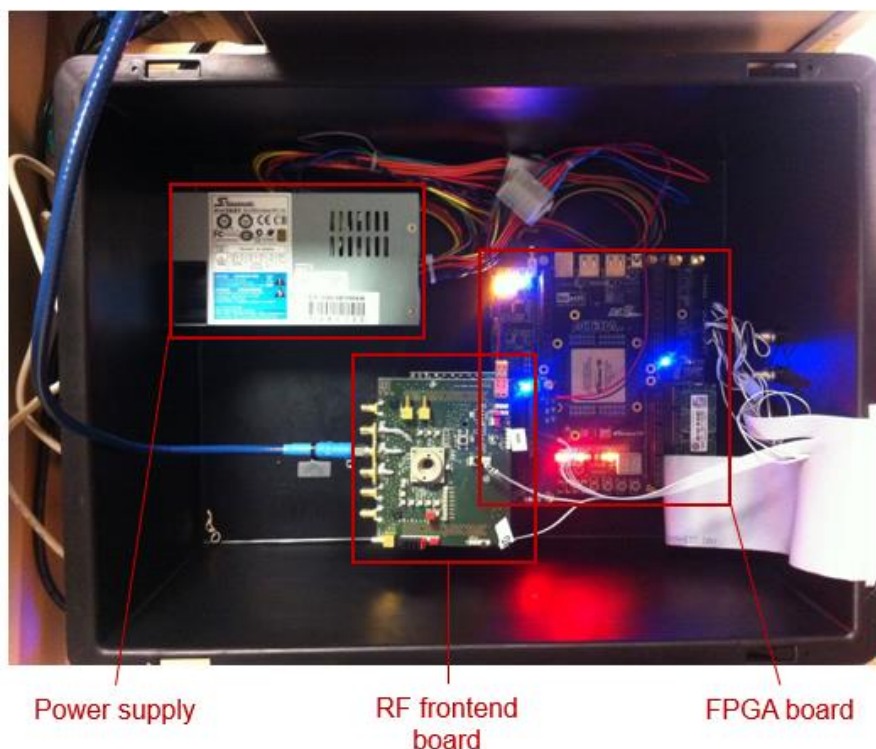


Figure 65: Top view of the core hardware blocks

The level shifter board is not visible in this illustration because it is stacked underneath the frontend board to mitigate the loss between the several ADC interfaces. On the right hand side of the picture one can see the ribbon cable connecting all the necessary interfaces to the TestStation. Additionally the RF cable

connecting the frontend evaluation board with the signal generator is visible on the left side.

The next picture shows the complete FPGA verification setup with all its components (except the host PC).

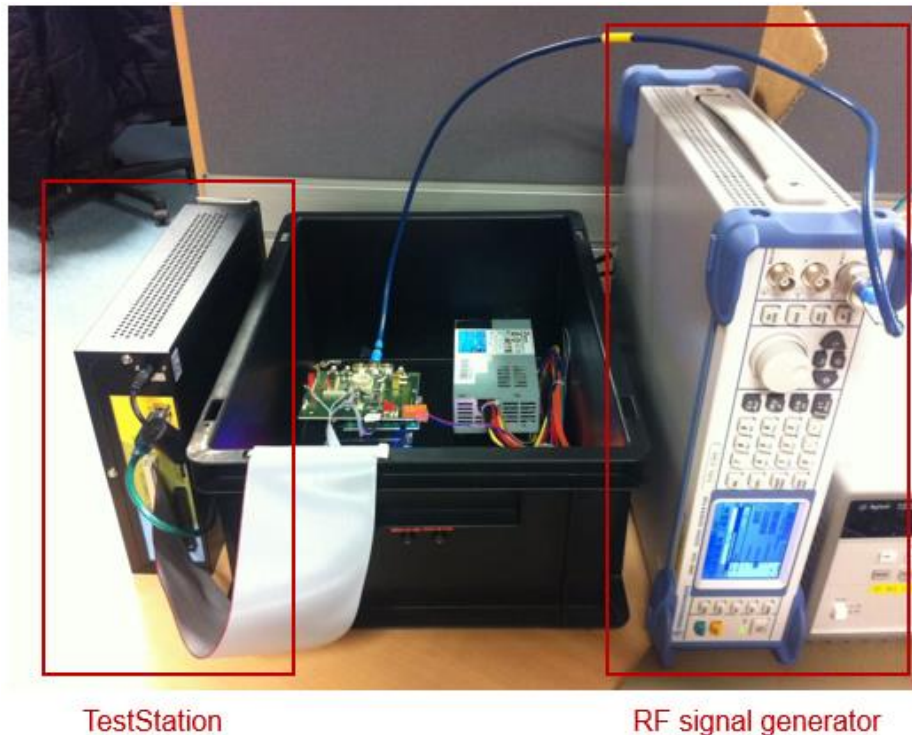


Figure 66 : Illustration of the complete FPGA verification setup

One can see the TestStation connected to all the necessary interfaces via a ribbon cable as well as the RF signal generator connected to the frontend evaluation board. For a better overview, the connection between the signal generators external modulation input and the connectors on the front side of the FPGA box was not placed. During the application a coaxial cable connects these two interfaces.

5.2 Configuration files

This section illustrates how the FPGA test bench is configured. For both, the sensitivity and for the jammer measurement test cases, Extensible Markup Language (XML) files are used for the configuration input.

5.2.1 Sensitivity measurements

Following image illustrates how a configuration file for the sensitivity measurement test case looks like. It contains all the necessary information about the use case (e.g. chip rate, FSK deviation, etc.) as well as the transmit frequency and the paths to the input and output directories.

```
<Session>
  <Sensitivity-Measurement
    DisplayName="Sensitivity Measurement"
    SendWupBeforeFrame="False"
    ModulationTypeSel="FSK"
    DigitalConfig="UseCase_CTC599__Dv1200Cr1200.bf"
    OutputDirectory="Instant_Output"
    UseCaseId="599"
    FskDeviation="1200"
    TxFrequency="925000000"
    ChipRate="1200"
    AnalogConfig="phcaiMtcRx925M0.bf"
  />
</Session>
```

Figure 67: Extraction of a sensitivity configuration file

This block of configuration is only the input for one use case. In order to test all use cases consecutively, this block must be copied for each use case. Of course the use cases dependent settings have to be adapted for each block.

5.2.2 Jammer measurements

The configuration of the jammer measurement test cases is very similar to the one of the sensitivity test case above. But of course some additional information about the jammer type and the jammer RF parameters are necessary.

```
<Session>
  <Jammer-Measurement
    DisplayName="UC599_AM"
    ModulationType_RX="FSK"
    ModulationType_Jammer="AM"
    DigitalConfig="UseCase_CTC599__Dv1200Cr1200.bf"
    UseCaseId="599"
    FskDeviation_RX="1200"
    TxFrequency="925000000"
    ChipRate_RX="1200"
    DataRate_Jammer="200"
    AnalogConfig="phcaiMtcRx925M0.bf"
  />
</Session>
```

Figure 68: Extraction of a jammer measurement configuration file

5.3 Result files

The different type of output files generated by the FPGA setup is documented in this section of the study. Those files can be opened in result viewers or converted to Excel format with a self-written export tool.

5.3.1 Sensitivity measurements

The raw output format of the sensitivity measurement test case is a tabulator separated text file with the extension *.dat*. This format was chosen to make it readable already in the raw format. The picture below shows an extract of such a file.

Input Signal	Meas.Cnt.	Meas Type	FER [%]	SyncFail [%]	DataFail [%]	Level [dBm]	Protocol ID	BIT_MODE	UseCase_ID
FSK	100	Sensitivity	100	100	0	-130	1	1	599
FSK	100	Sensitivity	67	3	64	-125	1	1	599
FSK	100	Sensitivity	30	1	29	-123.75	1	1	599
FSK	100	Sensitivity	23	0	23	-123.125	1	1	599
FSK	100	Sensitivity	17	0	17	-122.8125	1	1	599
FSK	100	Sensitivity	9	0	9	-122.5	1	1	599
FSK	100	Sensitivity	0	0	0	-120	1	1	599
FSK	100	Sensitivity	0	0	0	-110	1	1	599

Figure 69: Extraction of a raw sensitivity result

5.3.2 Jammer measurements

As the jammer measurement test case produces lots of data anyhow, it would not make sense to look at the data in raw format. Thus the XML format was chosen for the raw data. The figure below shows an extract of such a XML file.

```
<ResultPerDevice Id="2">
  <Name>Blocking Level</Name>
  <Value>-83</Value>
  <Unit>dB</Unit>
  <ForceValue>10000000</ForceValue>
  <ForceUnit>Hz</ForceUnit>
</ResultPerDevice>
```

Figure 70: Extraction of a raw jammer measurement result

5.4 Result viewer

In order to look at the gathered results in a visual way, result viewers are implemented that can read and open the raw results files described earlier. Two different result viewers are available, one for the sensitivity results and one for the jammer measurement results.

5.4.1 Sensitivity measurements

Once the result viewer is opened and some results were loaded, a window like shown in the picture below will be visible.

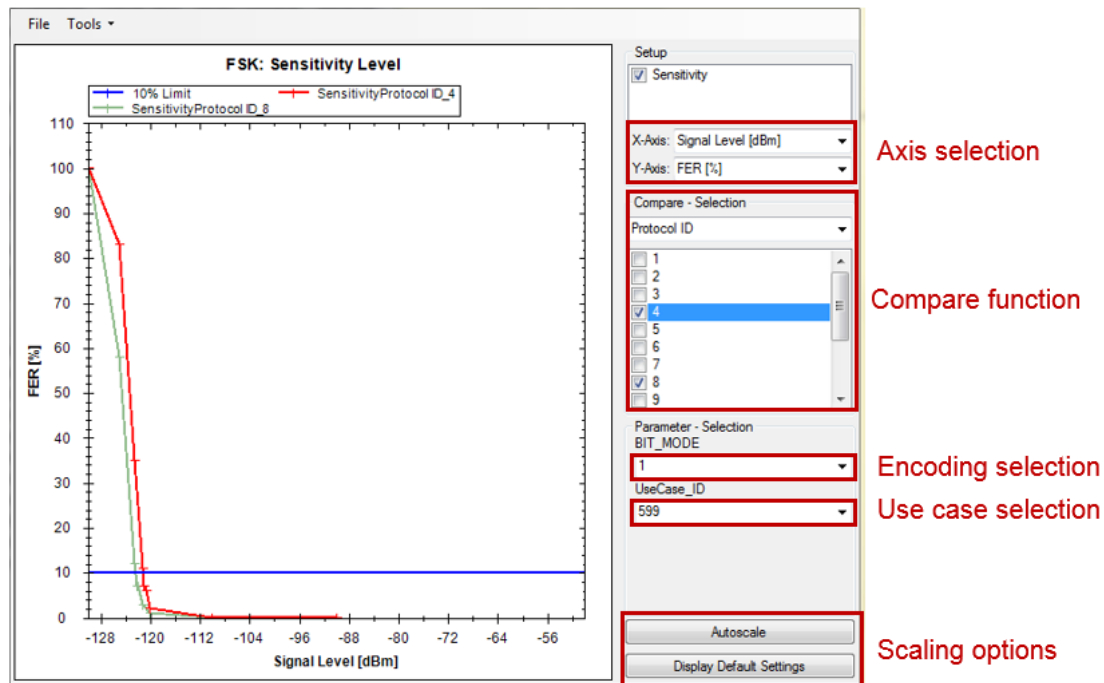


Figure 71: Sensitivity result viewer

The viewer contains of a main display window, which is scalable by mouse actions like scrolling or selecting and a number of filtering and compare functions. The user is able to select what is printed on the two different axes, which results should be compared to each other and how the selection of the remaining parameters should look like.

Additionally the user is able to easily store the actual view by clicking the right mouse button and selecting *Save Image* in the context menu.

5.4.2 Enhanced sensitivity measurements

Furthermore, the same result viewer is able to open the results of the enhanced sensitivity measurement test case with sweeps over the center frequency offset, the FSK deviation or the chip rate.

The picture below illustrates how these results can be displayed. In the case below, the sweep over the center frequency offset was chosen to be the x-axis and two different input levels are compared to each other.

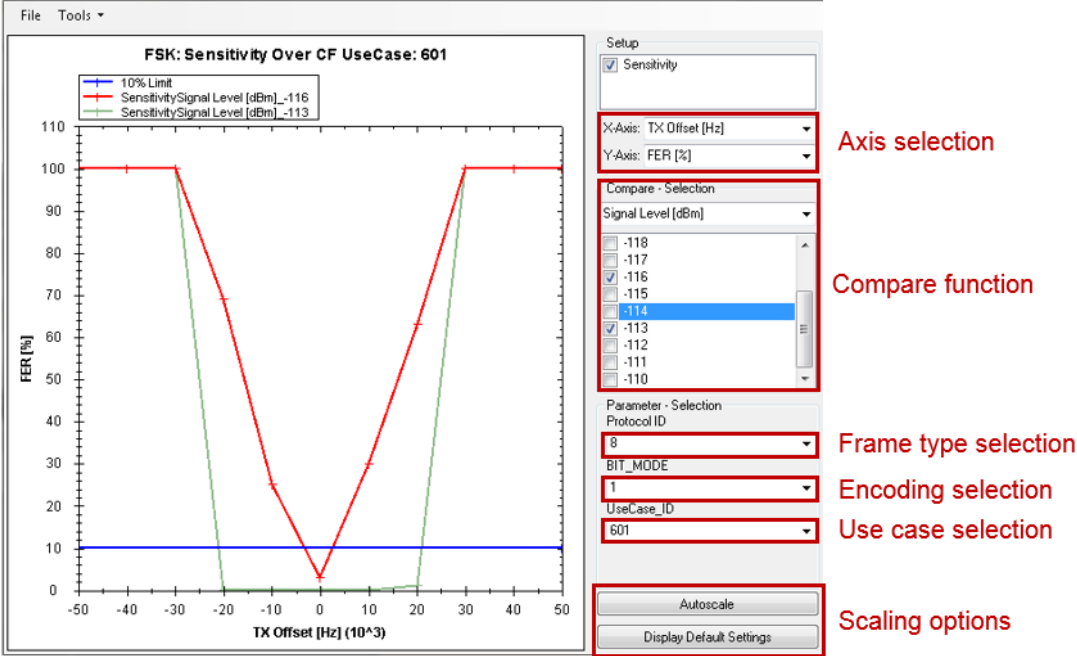


Figure 72: Enhanced sensitivity result viewer

As one can see, the result viewer is written to be hundred percent generic and free configurable by the user.

5.4.3 Jammer measurements

The result viewer for the jammer measurement looks very similar to the one of the sensitivity test case. The background though is very different because the input format of the results files is XML instead of the tabulator separated text files.

Like for the viewers described earlier, the windows consists of a scalable display window where the results are shown and a menu bar on the right side of the viewer. Also in this case saving images via the context menu is possible.

The menu bar on the right side of the viewer contains two boxes for filtering and comparing the loaded results. Furthermore a section for scaling options is implemented.

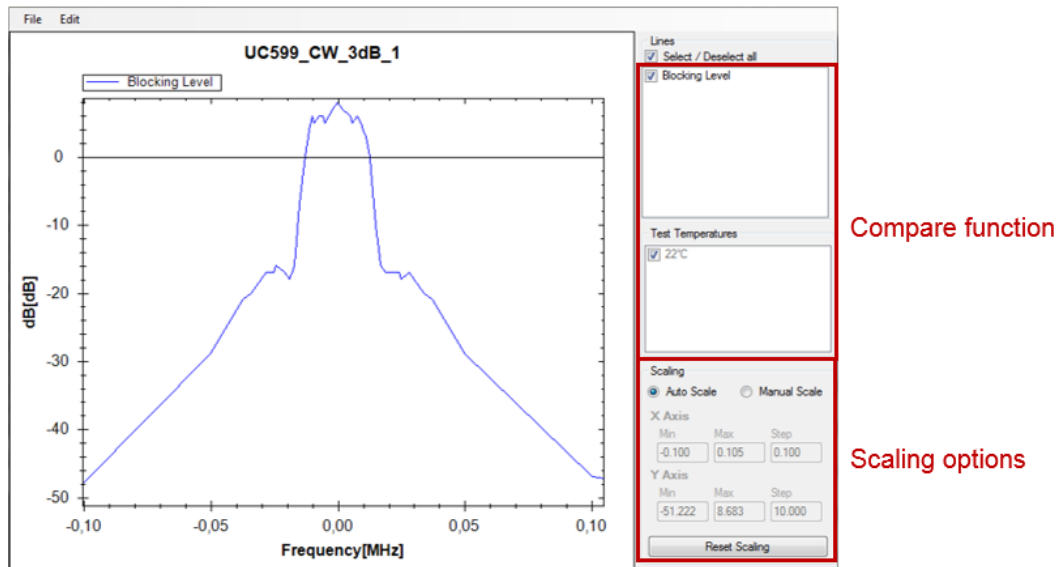


Figure 73: Jammer measurement result viewer

As one can see, also this viewer is built for maximum convenience of the user by offering lots of filter and display options.

5.5 Excel export

This section will show, how the results files in raw format can be converted to nice Excel sheets for reporting.

5.5.1 Sensitivity measurements

To generate a nice, colorful Excel sheet, only a few steps from the user are necessary. First one has to load all the results to export in the result viewer shown earlier, afterwards the context menu contains an entry to open the export GUI shown in the figure below

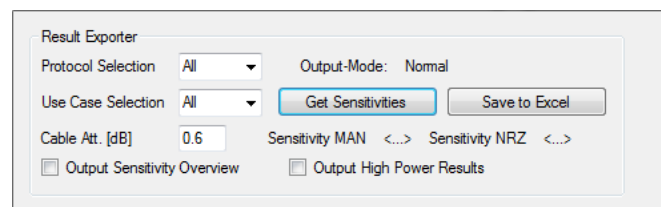


Figure 74: Export GUI for the sensitivity results

By clicking on the *Save to Excel* button on the right side of the window, the export tool generates an Excel sheet with a set of data like shown in the next figure.

	Protocol 5		Protocol 6		Protocol 7		Protocol 8		Protocol 9		Protocol 10		Protocol 11		Protocol 12		Protocol 13		Protocol 14		Protocol 15	
	NRZ	MAN	NRZ	MAN	NRZ	MAN	NRZ	MAN	NRZ	MAN	NRZ	MAN	NRZ	MAN	NRZ	MAN	NRZ	MAN	NRZ	MAN	NRZ	MAN
UC599	-121	-124	-121	-124	-121	-123	-121	-124	-121	-123	-121	-122	-121	-123	-121	-123	-121	-124	-121	-123	-121	-124
UC600	-118	-121	-118	-121	-120	-120	-118	-120	-119	-119	-117	-120	-118	-120	-118	-120	-118	-121	-117	-121	-119	-121
UC601	-114	-117	-114	-117	-115	-117	-114	-116	-115	-117	-114	-115	-114	-116	-115	-116	-114	-117	-115	-116	-114	-117
UC602	-113	-116	-113	-116	-113	-115	-113	-116	-113	-114	-113	-114	-113	-114	-113	-115	-113	-116	-113	-116	-113	-116
UC603	-109	-111	-110	-111	-110	-111	-109	-111	-110	-110	-109	-110	-110	-111	-109	-111	-109	-111	-109	-111	-110	-111
UC604	-108	-109	-107	-108	-106	-108	-104	-109	-104	-104	n.b.l.	n.b.l.	-107	-106	-106	-106	-106	-108	-107	-108	-107	-109
UC605	-105	-107	-104	-105	-100	-104	-103	-106	-103	-104	n.b.l.	-106	-101	-101	-102	-102	-101	-104	-101	-104	-104	-106
UC606	-117	-119	-118	-120	-118	-120	-117	-119	-118	-119	-117	-118	-118	-119	-117	-119	-118	-120	-117	-119	-118	-120
UC607	-110	-113	-110	-113	-110	-113	-110	-113	-110	-111	-110	-112	-110	-112	-111	-112	-110	-113	-110	-113	-110	-114
UC616	-111	-114	-111	-114	-111	-113	-111	-113	-111	-112	-111	-112	-111	-112	-111	-112	-111	-113	-111	-113	-112	-113
UC619	-105	-106	-104	-105	-105	-106	-105	-106	-105	-105	-106	-106	-105	-105	-105	-105	-104	-106	-105	-106	-106	-106
UC620	-112	-114	-112	-115	-112	-114	-112	-114	-112	-114	-112	-114	-112	-114	-112	-113	-113	-114	-112	-114	-112	-114
UC621	-109	-109	-108	-109	-109	-109	-108	-109	-109	-109	-110	-109	-110	-109	-110	-109	-109	-109	-109	-109	-109	-110
UC622	-115	-115	-115	-115	-115	-115	-115	-115	-115	-115	-114	-115	-115	-115	-115	-115	-115	-115	-115	-115	-115	-115
UC623	-112	-112	-112	-112	-111	-112	-112	-112	-112	-112	-112	-112	-112	-112	-112	-112	-111	-112	-112	-112	-112	-112
UC624	-108	-108	-107	-108	-107	-108	-107	-108	-107	-107	-108	-107	-108	-107	-107	-107	-107	-107	-107	-108	-108	-108

Figure 75: Extraction of an exported set of sensitivity results

As the handling of conditional formatting by automatically generated Excel sheets is quite complex, this set of data does not contain any formatting. The data has to be copied manually in a prepared master template containing all the conditional formatting as well as the limits. The picture below shows an extract of the result file after copying the data into the master template.

	Protocol 5		Protocol 6		Protocol 7		Protocol 8		Protocol 9		Protocol 10		Protocol 11		Protocol 12		Protocol 13		Protocol 14		Protocol 15		Limits [dBm]	
	NRZ	MAN	NRZ	MAN	NRZ	MAN	NRZ	MAN	NRZ	MAN	NRZ	MAN	NRZ	MAN	NRZ	MAN	NRZ	MAN	NRZ	MAN	NRZ	MAN	NRZ	MAN
UC599	-121	-124	-121	-124	-121	-123	-121	-124	-121	-123	-121	-122	-121	-123	-121	-123	-121	-124	-121	-123	-121	-124	-117	-120
UC600	-118	-121	-118	-121	-120	-120	-118	-120	-119	-119	-117	-120	-118	-120	-118	-120	-118	-121	-117	-121	-119	-121	-116	-119
UC601	-114	-117	-114	-117	-115	-117	-114	-116	-115	-117	-114	-115	-114	-116	-115	-116	-114	-117	-115	-116	-114	-117	-113	-116
UC602	-113	-116	-113	-116	-113	-115	-113	-116	-113	-114	-113	-114	-113	-114	-113	-115	-113	-116	-113	-116	-113	-116	-111	-114
UC603	-109	-111	-110	-111	-110	-111	-109	-111	-110	-110	-109	-110	-110	-111	-109	-111	-109	-111	-110	-111	-109	-111	-106	-109
UC604	-108	-109	-107	-108	-106	-108	-104	-109	-104	-104	n.b.l.	n.b.l.	-107	-106	-106	-106	-106	-108	-107	-108	-107	-109	-105	-108
UC605	-105	-107	-104	-105	-100	-104	-103	-106	-103	-104	n.b.l.	-106	-101	-101	-102	-102	-101	-104	-101	-104	-104	-106	-100	-103
UC606	-117	-119	-118	-120	-118	-120	-117	-119	-118	-119	-117	-118	-118	-119	-117	-119	-118	-120	-117	-119	-118	-120	-114	-117
UC607	-110	-113	-110	-113	-110	-113	-110	-113	-110	-111	-110	-112	-110	-112	-111	-112	-110	-113	-110	-113	-110	-114	-108	-111
UC616	-111	-114	-111	-114	-111	-113	-111	-113	-111	-112	-111	-112	-111	-112	-112	-112	-111	-113	-111	-113	-112	-113	-108	-111
UC619	-105	-106	-104	-105	-105	-106	-105	-106	-105	-105	-106	-106	-105	-105	-105	-105	-104	-106	-105	-106	-106	-106	-103	-106
UC620	-112	-114	-112	-115	-112	-114	-112	-114	-112	-114	-112	-114	-112	-114	-112	-113	-113	-114	-112	-114	-112	-114	-109	-112
UC621	-109	-109	-108	-109	-109	-109	-108	-109	-109	-109	-110	-109	-110	-109	-109	-109	-109	-109	-109	-109	-109	-110	-104	-107
UC622	-115	-115	-115	-115	-115	-115	-115	-115	-115	-115	-114	-115	-115	-115	-115	-115	-115	-115	-115	-115	-115	-115	-111	-114
UC623	-112	-112	-112	-112	-111	-112	-112	-112	-112	-112	-112	-112	-112	-112	-112	-112	-111	-112	-112	-112	-112	-112	-107	-110
UC624	-108	-108	-107	-108	-107	-108	-107	-108	-107	-107	-108	-107	-108	-107	-107	-107	-107	-107	-107	-108	-108	-108	-103	-106

Figure 76: Extraction of the set of sensitivity results in the master template

Such templates and export options are available also for all enhanced sensitivity measurements, meaning the sweep over the chip rate offset, the center frequency offset or the FSK deviation offset.

5.5.2 Jammer measurements

The export of the jammer measurement results works a bit different compared to the process for the sensitivity results. As much more data has to be handled, a dedicated export and filtering GUI was implemented. This GUI is shown in the next picture and has the most important sections marked in red.

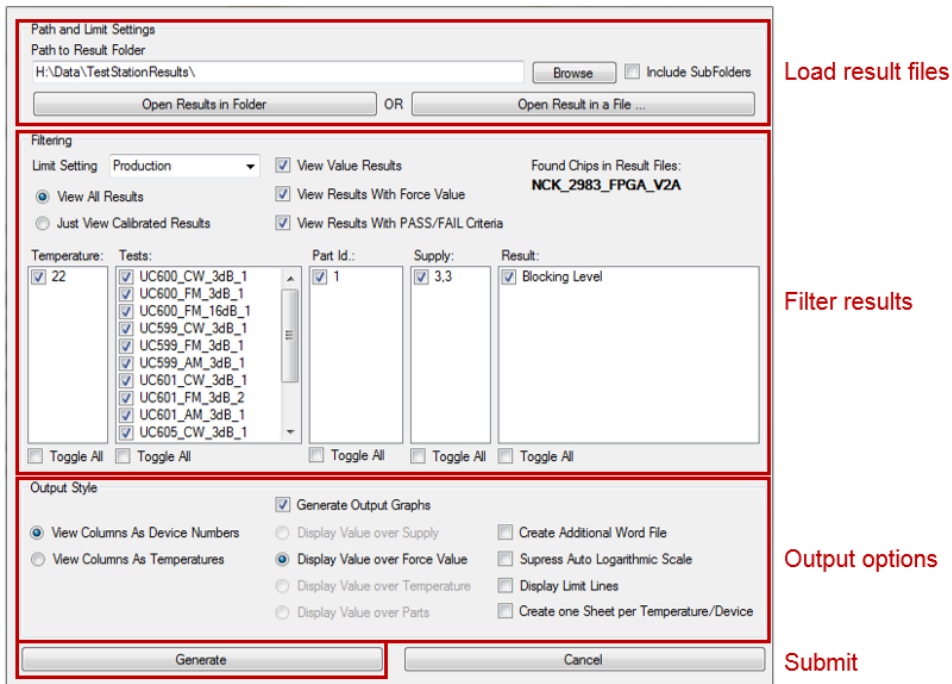


Figure 77: GUI for converting jammer measurement results to Excel

After loading and filtering all the results that should be saved to an Excel workbook, the *Generate* button at the bottom of the window has to be clicked. Following figure illustrates an extract of the output of this export GUI.

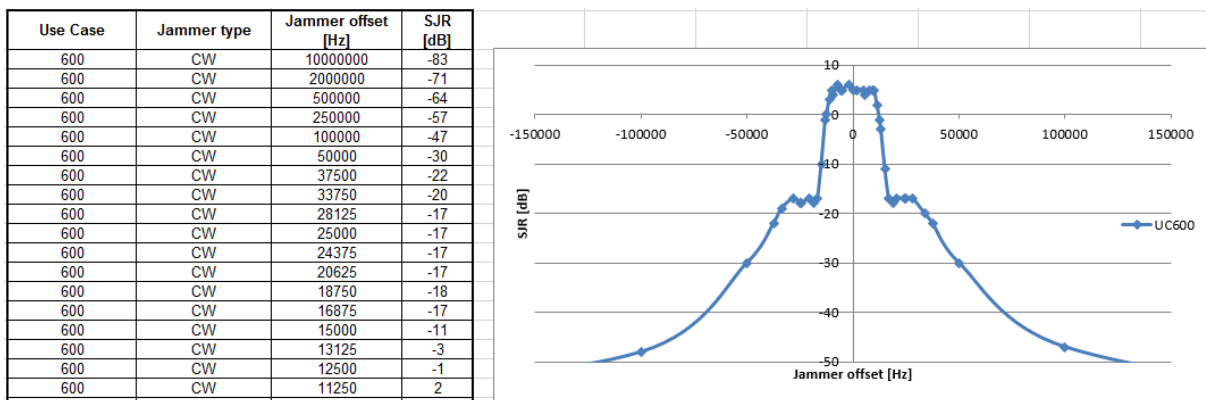


Figure 78: Extraction of the generated jammer measurement Excel result

The export tool automatically creates an Excel workbook that contains all the raw data in a readable format as well as plots of the signal to jammer ratio over the jammer offset frequency for each use case and jammer type.

6. Conclusion and outlook

To sum up this study, this section gives an overview about the gained conclusions and about the decision how to go on with the implemented FPGA setup. First the results of the comparison with the real silicon IC are presented, which are decisive for the success of this setup, afterwards possible enhancement options are presented. Finally the portability of the setup to future products is discussed.

6.1 Comparison FPGA / IC

Like written earlier, the FPGA system already emulates the final IC. Therefore the test bench and its configurations can be fully reused for the verification of the silicon. The only thing that has to be updated, are the potential changes in the configuration of the analog front end compared to the one which was used for the FPGA verification. But except this small part, everything is plug and play once the IC arrives. Therefore no double work is needed and the bring-up phase of the IC can be very short.

Of course one of the first actions after the silicon arrived was to start the same verification that was done on the FPGA also on the real IC. Fortunately the results nearly match perfectly! Following figure shows an extract of the comparison of the results from of the FPGA compared the results of the silicon.

	Protocol 4		Protocol 5		Protocol 6		Protocol 7		Protocol 8		Protocol 9		Protocol 10		Protocol 11		Protocol 12		Protocol 13		Protocol 14		Protocol 15	
	NRZ	MAN	NRZ	MAN	NRZ	MAN	NRZ	MAN	NRZ	MAN	NRZ	MAN	NRZ	MAN	NRZ	MAN	NRZ	MAN	NRZ	MAN	NRZ	MAN	NRZ	MAN
UC599	0.5	0.6	0.1	1.4	0.2	0.5	0.5	1.4	0.9	1.3	1.3	0.9	0.8	0.7	1.1	0.8	0.5	1.6	0.7	1.4	0.0	0.8	0.4	1.5
UC600	1.1	1.0	0.0	0.3	0.4	1.5	1.6	-0.1	1.1	0.7	1.4	-0.2	0.3	0.3	-0.2	0.2	0.5	0.5	1.8	0.3	1.2	1.1	0.4	
UC601	0.8	0.8	-0.4	0.5	0.1	0.6	1.5	0.9	0.3	-0.2	0.5	0.6	0.0	0.3	0.1	0.9	0.0	-0.5	0.1	0.3	1.6	-0.3	0.5	1.0
UC602	0.8	0.5	0.5	0.9	0.7	1.4	0.8	0.5	0.9	0.9	0.4	0.5	0.6	0.9	0.4	0.8	1.0	1.7	1.1	1.3	0.8	0.8	1.0	1.4
UC603	0.5	1.0	0.1	0.7	0.5	0.3	1.3	0.5	-0.3	0.4	0.7	0.6	0.3	0.1	0.6	0.8	0.2	0.6	-0.4	0.8	0.9	0.6	0.4	0.5
UC606	0.5	0.7	0.1	0.0	0.3	0.1	0.2	0.1	0.6	-0.1	0.6	0.5	0.3	-0.3	1.1	0.6	1.0	-0.2	0.7	0.5	0.6	-0.1	0.5	0.8
UC607	0.3	1.0	0.7	0.1	0.6	0.6	0.4	0.0	0.0	0.4	-0.2	0.4	0.5	1.1	-0.3	0.2	1.8	0.3	0.6	0.0	-0.2	0.3	0.5	1.1
UC616	1.0	0.9	1.0	0.6	0.1	0.8	0.7	0.3	0.2	0.6	0.5	1.3	0.8	0.5	0.3	-0.7	0.8	0.4	0.3	0.0	0.6	0.3	1.3	-0.1
UC620	1.2	0.8	0.4	0.4	-0.1	0.8	0.5	0.2	0.6	0.0	0.3	1.1	0.6	0.6	0.6	1.2	0.1	0.5	1.0	0.5	0.6	0.6	-0.2	0.1
UC621	0.7	0.7	1.4	0.4	0.6	0.6	0.9	0.1	0.9	0.8	1.1	0.5	0.4	0.8	0.7	1.1	1.5	-0.2	1.4	-0.1	0.6	0.6	0.8	0.3
UC622	0.6	0.4	0.4	0.5	0.5	0.4	0.4	0.5	0.3	0.8	0.5	0.6	0.2	-0.7	0.5	0.5	0.8	0.5	0.5	0.4	0.4	0.5	0.5	0.5
UC623	0.5	0.6	0.7	0.5	0.4	0.6	0.6	0.7	0.6	0.5	0.5	0.4	1.2	0.6	0.8	0.5	0.5	0.4	0.5	0.4	0.5	0.3	0.7	0.5
UC624	0.3	0.4	0.5	0.3	0.3	0.5	0.6	0.5	0.6	0.5	-0.2	0.3	0.4	0.5	0.4	0.7	0.4	0.5	0.5	0.4	0.6	0.5	0.5	0.3
UC629	0.7	-1.0	0.8	1.0	1.3	0.6	0.9	-0.1	0.5	0.2	1.0	0.7	0.0	0.2	0.9	0.3	1.1	0.8	1.3	0.6	0.6	0.6	1.0	0.5
UC630	1.2	0.5	0.3	0.8	0.8	0.3	0.0	0.6	0.7	-0.1	0.5	0.8	1.1	0.1	0.9	0.6	0.6	0.6	0.8	0.4	0.7	0.5	0.7	0.5
UC631	0.8	0.8	0.9	0.3	0.0	0.6	0.5	0.2	0.7	0.2	0.5	0.8	0.7	1.0	0.8	0.2	0.0	-0.3	0.9	0.5	0.3	0.4	0.6	1.3
UC632	0.9	0.2	0.8	0.3	0.6	0.6	0.3	0.9	0.5	0.3	0.5	0.8	-2.2	-1.0	0.3	0.8	0.8	0.0	0.7	1.8	1.1	0.2	1.0	0.3
UC633	0.6	0.5	0.3	0.4	0.4	0.3	0.4	0.5	0.8	0.3	0.2	0.6	0.4	0.5	0.5	0.7	0.3	0.4	0.6	0.6	0.6	0.5	0.5	0.5
UC634	0.1	-0.1	-0.2	1.4	0.4	0.1	1.8	0.7	0.7	0.5	1.4	0.3	0.7	0.1	0.7	0.3	0.7	0.2	0.3	0.8	0.6	0.3	0.3	0.5
UC635	0.8	0.0	0.8	0.3	0.7	1.3	0.5	0.5	0.0	0.3	1.1	0.5	0.5	0.6	1.0	1.1	0.6	0.5	0.8	0.6	1.1	0.9	1.0	0.9
UC636	0.3	1.1	0.8	0.0	0.7	0.6	0.9	0.9	0.7	0.7	0.8	0.5	0.4	0.6	1.1	0.8	-0.2	1.1	0.4	0.8	0.6	0.1	0.5	-0.1

Figure 79: Extract of the comparison between the FPGA and the final IC

These results prove the reliability of the system and strengthened the idea, to verify from now onwards every receiver with such a FPGA setup.

6.2 Capturing of ADC streams

For test and debugging purposes the FPGA implementation has been enhanced by a special recording and playback mechanism that allows in-system injection and monitoring of a set of pre-defined signals. Although the development of this feature originally was intended to be used for the spread spectrum sub-block (DSSS), it could also be re-used for injection of the ADC I & Q data streams, as well as for recording of the receive debug bus. In addition, a Quartus Signaltap [22] core has been inserted for tracking of various important signals, e.g. CPU program counter, ports, interrupt signals, etc.

All these functionalities are already available in the FPGA implementation and could be accessed by the host software. One possible implementation could be, that the TestStation is used to trigger the recording of the ADC I & Q data streams via an IO channel. Afterwards the host software could read out the recorded stream and display it visually in a nice GUI on the host PC. This would enable lots of additional debugging functionalities if one would like to know why dedicated frames cannot be correctly demodulated by the receive chain.

6.3 Measurement time optimizations

As the available time for the verification of a receiver before the design freeze happens is always very limited, the measurement time is the key to success. If the time to measure the frame error rate can be reduced, the measurement coverage can be even increased without increasing the verification time.

One possible option would be to transfer a part of the frame error rate measurement into a firmware which is executed by the micro controller synthesized in the FPGA. A big time consumer is the communication with the IC before and after each frame. The actual system is built in a way that the received payload is read out after each sent frame. This is needed for the comparison of the sent data with the received data. As the communication speed is quite low and also the number of TestStation commands needed is high and furthermore hundreds of frames have to be sent until the sensitivity limit is distinguished, this takes quite a long time.

If all the payloads that are going to be sent are passed to the firmware of the IC before the transmission starts and the comparison of the received payload with the sent data is done internally by the micro controller, the measurement time could be reduced tremendously. The number of communications between the TestStation and the IC in the FPGA would be reduced heavily which saves a lot of measurement time.

Furthermore a smart way of detecting the sensitivity level could be introduced. Actually a static number of one hundred frames is sent per power level to check if the frame error rate is above or below ten percent. But if all or no frames are correctly demodulated, ten frames also would have been enough to take the right decision. Only in the range of the sensitivity limit plus minus 3dB one hundred frames are necessary to get an accurate result. By implementing such a smart way of measuring the frame error rate efficiently, a lot of wasted time can be saved.

6.4 Portability to future prototypes

Like written in previous chapters. the prerequisite of such a FPGA based verification is of course, that the analog front end of the receiver to be verified is either already available on a test chip, or does not change tremendously compared to the previous version of the receiver. This is the case because a verification of the digital part of the receiver makes no sense, if the analog part (e.g. the Sigma Delta ADC) changes dramatically. Aim of the FPGA based verification is to test the whole system, frontend as well as backend.

Luckily NXP will never tape a completely new product without carrying out the verification on a test chip before, especially if lots of hardware IPs change. The only exception is, if a product differs only in a few aspects compared to the previous one, in that case a test chip verification can be disclaimed. In both cases, a frontend IC for a FPGA verification is available. Therefore this kind of verification of the digital receive chain can be carried out for all future types of NXPs receivers.

As the verification of the receiver for which the setup was built, was very successful, already two more receiver versions were ported to the FPGA test bench. One of them is also already finished successfully, the second one is actually in progress.

References

1. NXP, *ATIC134 Medium Datasheet*. 2013.
2. Friis, H.T. and J.R. Pierce, *The Wisdom of Harald Friis*. 1957.
3. Friis, H.T., *Noise Figures of Radio Receivers*. Proceedings of the IRE, 1944. **32**(7): p. 419-422.
4. Sabah, S. and R. Lorenz. *Design and calibration of IQ-Mixers*. in *EPAC*. 1998.
5. Tietze, U. and C. Schenk, *Halbleiter-Schaltungstechnik: [neuer Teil: Nachrichtentechnische Schaltungen]*. 2002: Springer.
6. Schreier, R. and G.C. Temes, *Understanding Delta-Sigma Data Converters*. 2004: Wiley.
7. Söderkvist, S., *Tidsdiskreta system: Exempelsamling*. 1980.
8. Pirsch, P., *Architekturen der digitalen Signalverarbeitung*. 1996: Teubner.
9. Smith, S.W., *The scientist and engineer's guide to digital signal processing*. 1997: California Technical Publishing. 625.
10. Bakshi, A.P.G.U.A., *Analog Integrated Circuits - Design And Applications*. 2009: Technical Publications.
11. North, D.O., *An Analysis of the factors which determine signal/noise discrimination in pulsed-carrier systems*. Proceedings of the IEEE, 1963. **51**(7): p. 1016-1027.
12. Turin, G.L., *An introduction to matched filters*. Information Theory, IRE Transactions on, 1960. **6**(3): p. 311-329.
13. Sklar, B., *Digital communications: fundamentals and applications*. 2001: Prentice-Hall PTR.
14. ETSI, *Electromagnetic compatibility and Radio spectrum Matters (ERM); Short Range Devices (SRD); Radio equipment to be used in the 25 MHz to 1 000 MHz frequency range with power levels ranging up to 500 mW; Part 1: Technical characteristics and test methods*. 2012.
15. Gu, Q., *RF System Design of Transceivers for Wireless Communications*. 2005: Springer.
16. Hickman, I., *Practical RF Handbook*. 2006: Elsevier Science.
17. Altera, *Cyclone II Architecture*. 2007.
18. Betz, V. *FPGA Architecture for the Challenge*. Available from: http://www.eecg.toronto.edu/~vaughn/challenge/fpga_arch.html.
19. Wolf, W., *FPGA-Based System Design*. 2004: Pearson Education.

20. Altera, *Stratix III FPGA: Lowest Power, Highest Performance 65- nm FPGA*.
21. Schwarz, R., *R&S SMB100A Operating Manual*.
22. Altera, *Quartus II Handbook Version 13.1*. 2013.

List of Figures

- Figure 1: Full receive chain [1]..... 9
- Figure 2: Analog Frontend [1]..... 10
- Figure 3: IQ Mixer [4]..... 11
- Figure 4: Transimpedance amplifier [5] 12
- Figure 5: Block diagram of a first order SD ADC [1] 14
- Figure 6: Block diagram of the IF preprocessing [1] 14
- Figure 7: Decimation filter with lowpass filter followed by down sampling [7] 15
- Figure 8: Lowpass filter with a cut off frequency of π/M [7] 15
- Figure 9: Example of a decimated signal [7]..... 16
- Figure 10: DC notch filter response [8] 16
- Figure 11: Block diagram of the narrowband receive chain [1]..... 18
- Figure 12: CORDIC algorithm process [8] 18
- Figure 13: Ideal low pass filter [9] 19
- Figure 14: Impulse response of ideal LPF [9] 20
- Figure 15: Filter weights $M=20, f_t=0.23$ [9] 20
- Figure 16: Formulas to calculate the filter weights [9]..... 21
- Figure 17: Frequency response of a real LPF using a rectangular window [9] 21
- Figure 18: Comparison of Hamming window and rectangular window [9] 21
- Figure 19 : BLock Diagram of a FSK Demodulation PLL [1]..... 23
- Figure 20: Transmitted data without additive white Gaussian noise [12] 24
- Figure 21: Received data with additive white Gaussian noise [12] 24
- Figure 22: Received data after the matched filter [12] 25
- Figure 23: Sample points on the received signal [12] 25
- Figure 24: Block diagram of the clock data recovery [1] 25
- Figure 25: Block diagram of the MRK3 CPU [1] 28
- Figure 26: Illustration of a typical MDI command including a response of the IC..... 30
- Figure 27: BER measurement setup 32
- Figure 28: Test Message for FER Measurement..... 33

Figure 29: Timing of Test Message	34
Figure 30: FER measurement setup.....	34
Figure 31 : Jammer measurement setup.....	35
Figure 32: Principle of the interferer measurement.....	36
Figure 33: Position of ACR interferer	37
Figure 34: Position of Co-Channel interferer	38
Figure 35: Illustration of the IRR measurement	38
Figure 36: Position of the image interferer.....	39
Figure 37: Position of the blocking interferer	40
Figure 38: Illustration of a spurious response measurement	41
Figure 39 : FSK modulation principle [13].....	42
Figure 40: ASK modulation principle [13].....	42
Figure 41: Block diagram of a configurable logic block [17].....	45
Figure 42: Connections in a switch box [18]	45
Figure 43: Block diagram of the FPGA implementation	50
Figure 44: Clock and reset generation.....	50
Figure 45: Block diagram of the hardware setup	52
Figure 46 : RF frontend evaluation board	54
Figure 47: Schematic of the level shifter board.....	55
Figure 48: Terasic DE3-150 board	55
Figure 49: Front panel of the SMB100A signal generator [21].....	57
Figure 50: Rear panel of the SMB100A signal generator [21]	57
Figure 51 : NXP made tool “TestStation”	58
Figure 52: Block diagram of the TestStation hardware	59
Figure 53: Internal structure of the TestStation.....	59
Figure 54: IO driver structure of the TestStation channels.....	60
Figure 55: Illustration of the output of the implemented command	61
Figure 56: Command to setup the RF data frame system	62
Figure 57: Command to trigger a frame transmission.....	62
Figure 58: Start window of the TestStation GUI.....	63

Figure 59: Block diagram of the frame error rate measurement	65
Figure 60: Block diagram of the sensitivity measurement.....	66
Figure 61: Flow chart of the sensitivity test case	68
Figure 62: Flow chart of the enhanced sensitivity measurement	69
Figure 63: Block diagram of the signal to jammer ratio measurement	70
Figure 64: Flow chart of the interferer performance test case	71
Figure 65: Top view of the core hardware blocks	73
Figure 66 : Illustration of the complete FPGA verification setup	74
Figure 67: Extraction of a sensitivity configuration file	75
Figure 68: Extraction of a jammer measurement configuration file	75
Figure 69: Extraction of a raw sensitivity result.....	76
Figure 70: Extraction of a raw jammer measurement result	76
Figure 71: Sensitivity result viewer	77
Figure 72: Enhanced sensitivity result viewer	78
Figure 73: Jammer measurement result viewer.....	79
Figure 74: Export GUI for the sensitivity results.....	79
Figure 75: Extraction of an exported set of sensitivity results	80
Figure 76: Extraction of the set of sensitivity results in the master template.....	80
Figure 77: GUI for converting jammer measurement results to Excel	81
Figure 78: Extraction of the generated jammer measurement Excel result	81
Figure 79: Extract of the comparison between the FPGA and the final IC.....	82
Figure 80 : Schematic of the RF frontend evaluation board.....	91

List of Tables

Table 1: Channel filter selection 22

Table 2 : Use case overview..... 31

Table 3: Message protocol overview 33

Table 4 : Channel separation for each channel filter bandwidth 37

Table 5 : Implemented memories 51

Table 6: Necessary tools to implement a FPGA-ready bit stream 51

Table 7 : Detailed pinout of the FPGA evaluation board..... 92

Appendix A – RF frontend evaluation board

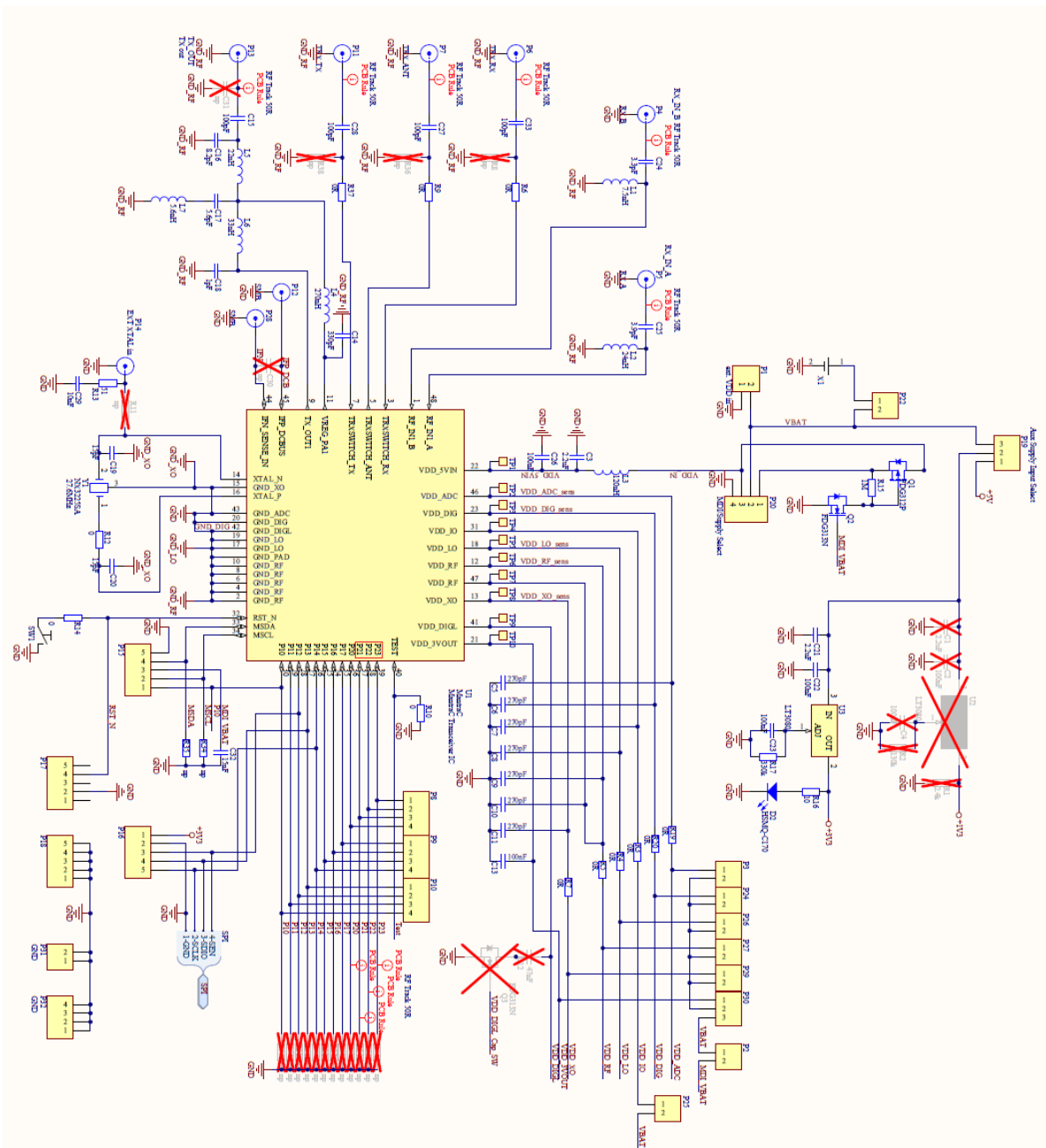


Figure 80 : Schematic of the RF frontend evaluation board

Appendix B – FPGA evaluation board

Table 7 : Detailed pinout of the FPGA evaluation board

Signal	FPGA Pin	Board Reference	Description
IOWmsda	AJ21	GPIO1_32	MDI MSDA (Data)
IwVbat	AP26	GPIO1_34	MDI Vbat
OwMscl	AP23	GPIO1_36	MDI MSCL (Clock)
IwBoardRst_an	U31	CPU_RESET	Board reset button
IwClk82mEn	W5	SW0	ADC Interface Enable (inverted). When in ON position, ADC I/Q/Clk are generated inside the FPGA. Thus, the THDB daughter board is not necessary in this case.
IwClk50m	W2	Y1	50 MHz oscillator
OwClk82m	B14	THDB-HTG J3 4	82 MHz clock output, to be used for loop back to IwAdcClock on a THDB daughter board. Switched on via SW0.
OLed0[0]	AD1	LED0/Red	Alive LED, toggling with approx. 1 sec period, based on System Clock (VddLoSysClk)
OLed0[1]	AB1	LED0/Green	Alive LED, toggling with approx. 1 sec period, based on DSSS Clock (IfClk)
IwAdcClock	B16	THDB-HTG J3 3	ADC Clock over daughter board connector J3
IwAdcl	D14	THDB-HTG J3 15	ADC I signal over daughter board connector J3
IwAdcQ	A11	THDB-HTG J3 16	ADC Q signal over daughter board connector J3
P14/ScIk	AE29	GPIO1_18	SPI Clk
P13/Sdio/Tx	AE30	GPIO1_16	SPI Data
P12/Sen/Rx	AF28	GPIO1_14	SPI Slave Select

			(enable)
P10	AD21	GPIO1_33	GPIO
P11	AE20	GPIO1_35	GPIO
P15	AJ20	GPIO1_28	GPIO (to be used only as output)
P17	AF21	GPIO0_40	GPIO
P16	AM22	GPIO1_31	GPIO ; RF Generator Trigger Output
P20	AG21	GPIO0_38	GPIO
P21	AN24	GPIO0_36	GPIO ; external DSSS Trigger Input
P22	AP24	GPIO0_34	GPIO
P23	AN22	GPIO0_32	GPIO
OLed4[0]	AG21	LED4	LED output of P20 (1 = ON)
OLed5[0]	AN24	LED5	LED output of P21 (1 = ON)
OLed6[0]	AP24	LED6	LED output of P22 (1 = ON)
OLed7[0]	AN22	LED7	LED output of P23 (1 = ON)
DacTestOut1	AP22	GPIO0_28	Bit 0
	AH33	GPIO0_26	Bit 1
	AG34	GPIO0_24	Bit 2
	AF31	GPIO0_22	Bit 3
	AF32	GPIO0_20	Bit 4
	AG31	GPIO0_18	Bit 5
	AG32	GPIO0_16	Bit 6
	AJ31	GPIO0_14	Bit 7
DacTestOut2	AJ32	GPIO0_10	Bit 0
	AH30	GPIO0_8	Bit 1
	AH31	GPIO0_6	Bit 2
	AL32	GPIO0_4	Bit 3
	AL33	GPIO0_2	Bit 4
	AL34	GPIO0_5	Bit 5
	AM34	GPIO0_7	Bit 6
	AK34	GPIO0_9	Bit 7
DacTest Clock	AK33	GPIO0_13	DAC Test Clock
DacTestEnable	AH34	GPIO0_15	DAC Test Enable
OwAdcl	AL23	GPIO0_39	ADC I debug output, sampled with neg. edge of ADC clock